Recent inland large lake outbursts on the Tibetan Plateau: Processes, causes and mechanisms

Fenglin Xu[1,2][†], Yong Liu[3][†], Guoqing Zhang[1], Ping Zhao[4], R. Iestyn Woolway[5],
Yani Zhu[6], Jianting Ju[1], Tao Zhou[1,2], Xue Wang[1,2], Wenfeng Chen[1]

[1]State Key Laboratory of Tibetan Plateau Earth System Science, Environment and Resources (TPESER),
Institute of Tibetan Plateau Research, Chinese Academy of Sciences, Beijing, China
[2]University of Chinese Academy of Sciences, Beijing, China
[3]Department of Atmospheric Science, School of Environmental Studies, China University of Geosciences,
Wuhan, China
[4]State Key Laboratory of Severe Weather, Chinese Academy of Meteorological Sciences, Beijing, China
[5]School of Ocean Sciences, Bangor University, Menai Bridge, Anglesey, UK
[6]National Meteorological Information Center, China Meteorological Administration, Beijing, China

[†]These authors contributed equally to this work.
Correspondence: Guoqing Zhang (guoqing.zhang@itpcas.ac.cn)

Abstract. Lake outburst events have been mainly focused on small glacial lakes in the Himalaya, while the historical events from inland large lakes are few and have received less attention. Inland large lakes on the Tibetan Plateau are expanding rapidly, with recent signs of increasing outburst risk, highlighting the need to elucidate the processes, causes and mechanisms to mitigate future impacts. Here, a long-term satellite lake mapping shows that the number and surface area of lakes on the Tibetan Plateau ~~show~~exhibit an increased trend over the past 50 years, ~~peaked~~ peaking in 2023~~, accompanied by t~~ Two notable outburst events occurred during this period: Zonag Lake (~150 km^2 in 2023) on 15 September 2011 and Selin Co (~2,465 km^2 in 2023, the largest lake in Tibet) on ~~23~~ 21 September 2023. The cascading outburst of Zonag Lake caused its area to shrink by ~124 km^2 (-45%), while the downstream Yanhu Lake expanded by ~163 km^2 (+347%). The Selin Co outburst resulted in a water ~~volume~~ mass loss of ~0.3 Gt, the downstream Bange Co experienced a water level rise of ~2.3 m and an area expansion of ~18%. Despite its large water storage capacity, Selin Co experienced less water loss due to the flat terrain at the breach and the slow flow (~1 m/s at the damaged road), with an average discharge of ~~~170~~ 154 m^3/s. Even with the low discharge, the Selin Co flood breached the lowland road within ~~~12~~ 10 hours. In contrast, the large breach and steep terrain at Zonag Lake facilitated a rapid discharge of a sustained volume of water, with an average discharge of ~2,238~~2,191~~ m^3/s. Selin Co resulted in only a short period of drainage reorganization, in contrast to the permanent reorganization caused by Zonag Lake. The underlying mechanisms of the increased precipitation as the main trigger for the two outburst events prior to the occurrence are different. For Zonag Lake, thermodynamic effects, i.e. changes in the atmospheric moisture, are the most important, while for Selin Co, dynamical effects, i.e. the vertical moisture motion induced by the changes in atmospheric circulation, dominate the precipitation patterns. Large lake outbursts in the Inner Tibetan Plateau are expected to increase in the near future due to the warmer and wetter climate, and urgent policy planning is needed to mitigate the potential future lake-induced flood damage.

1 Introduction

The Tibetan Plateau (TP) has the highest and most widely distributed cluster of ~~alpine~~ plateau lakes on Earth, with more than 1,400 lakes larger than 1 km^2 and a total area of ~50,000 km^2, accounting for more than half of China's lake surface area (Ma et al., 2010; Zhang et al., 2019a; 2019b). These alpine lakes serve as important sentinels of climate change and early warning signals of abrupt transitions in the Earth system (Lei et al., 2014; Zhou et al., 2021; Loewen, 2023; Chen et al., 2022). Between the 1970s and 1990s, a decreasing trend in lake area on the TP was observed, mainly due to decreasing precipitation. Subsequently, especially since the mid-1990s, a dramatic expansion of lake area has been detected~~observed~~, driven by increasing precipitation and a continuous increase in cryospheric meltwater (Zhang et al., 2017b; Song et al., 2013; Chen et al., 2022). The significant expansion of these lakes could ~~potentially~~ threaten ~~to~~ the fragile ecological environment of the TP, particularly by inundating grasslands, altering water resources, disrupting habitats, and impacting biodiversity (Xu et al., 2024).

However, the current glacial lake outburst floods (GLOFs) in the Himalaya have received considerable attention due to their extensive historical record and enormous downstream damage (Veh et al., 2020; Zheng et al., 2021). Outburst floods ~~(i.e., lake floods)~~ of large inland lakes (i.e., those far from the glaciers) in the TP have received less attention due to their relatively infrequent occurrence. Historically, the expansion of inland lakes has been cumulative, with few outbursts occurring due to thresholds or limits not being reached. However, in recent years, signs of lake outbursts have become increasingly apparent, accompanied by a continuous and dramatic increases in lake levels and outward expansion of lake boundaries (Lei et al., 2023; Liu et al., 2016).

~~For example, o~~On 15 September~~,~~ 2011, an outburst flood event occurred in the Zonag Lake located in the Hoh Xi region of the TP (Liu et al., 2016; 2019; Wang et al., 2022a; Lu et al., 2020a; 2021~~; Lu et al., 2020a~~). This outburst flood event altered the hydrological connectivity between lakes, linking Zonag Lake, downstream Kusai Lake, Hedin Noel Lake~~s~~ and Yanhu Lake (tailwater lake) (Lu et al., 2021; Chen et al., 2021b) (Figure 1). More recently, Selin Co, the largest lake in Tibet and the second largest lake in the TP, also experienced an outburst event on 24 21 September 2023, causing significant environmental and societal impacts. However, the processes and mechanisms behind these events are not well understood~~have not been well quantified~~. Overall, current studies~~research~~ lacks a comprehensive assessment~~,~~ and detailed examination ~~and comparison~~ of existing inland lake outburst events, which is essential to improve our knowledge~~understanding~~ of ~~inland~~ lake outburst and facilitate the development of early warning systems.
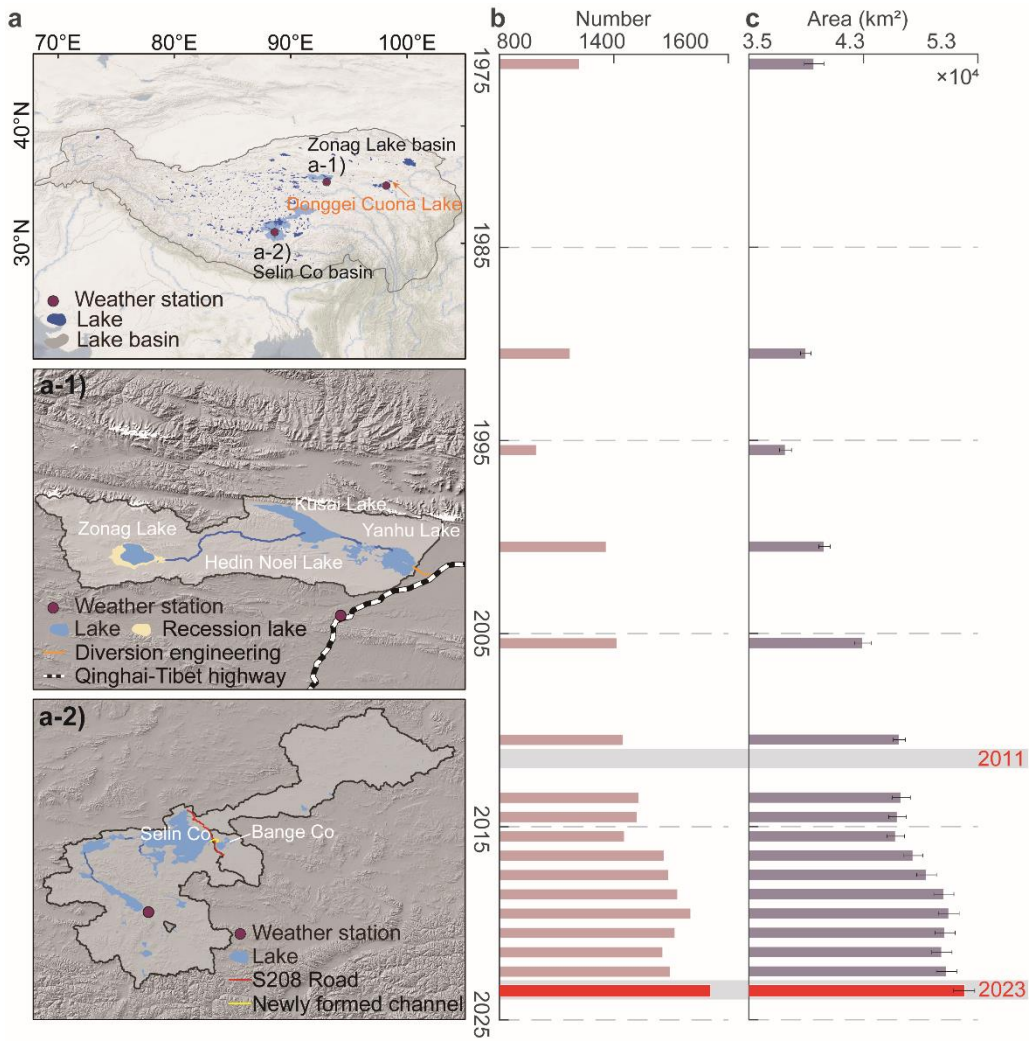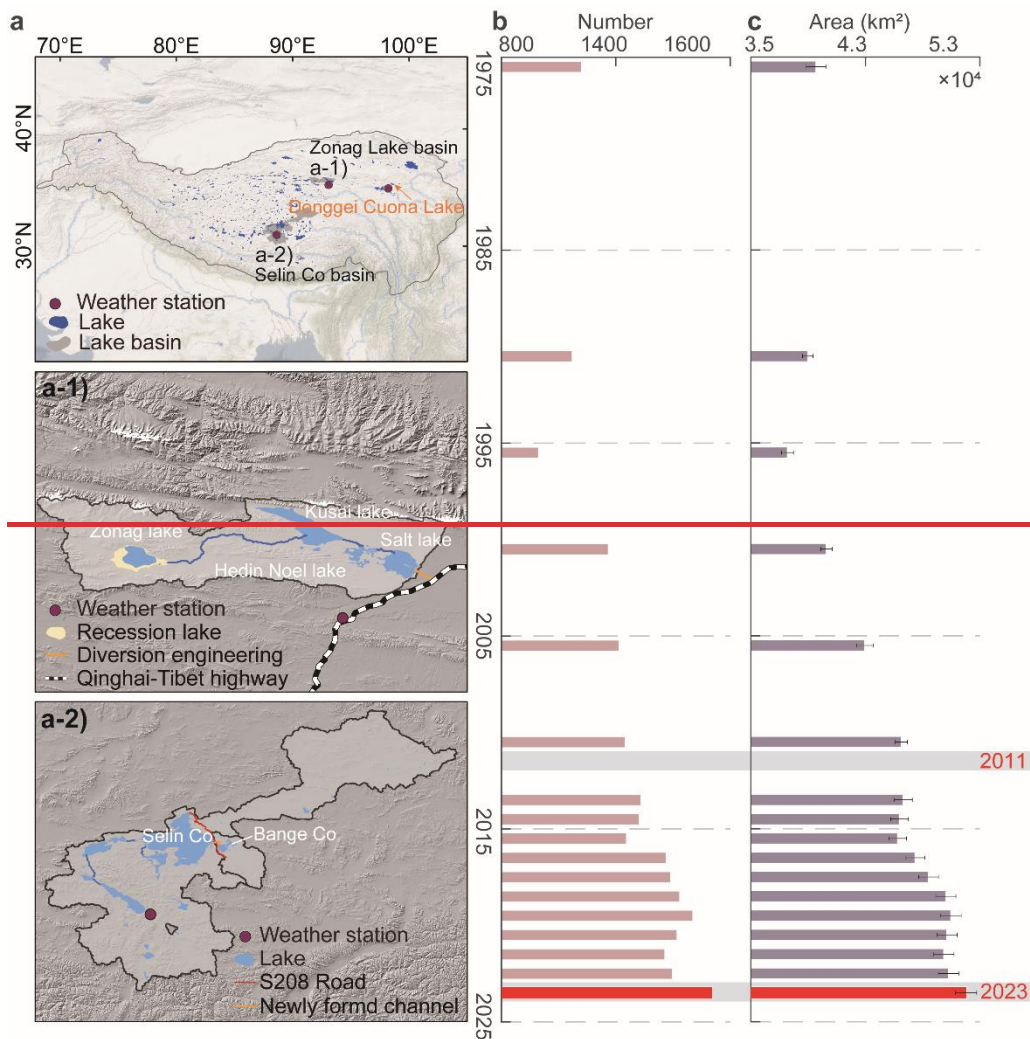
Figure. 1. Distribution and changes in number and area of lakes on the TP. (**a**) Location of the lakes on the TP, the Zonag Lake and Selin Co basin is shown in **a-1** and **a-2**. (**b**) Changes in the number of lakes (>1 km²). (**c**) Changes in area of lakes (>1 km²). Lake data from 1970 to —2018 data are come from Zhang et al. (2019a). Sources of background imagery for a): Esri, DigitalGlobe, GeoEye, i-cubed, USDA FSA, USGS, AEX, Getmapping, Aerogrid, IGN, IGP, swisstopo and the GIS User Community. Background image sources for a-1 and a-2: NASA JPL. NASADEM Merged DEM Global 1 arcsec V001. 2020, distributed by NASA EOSDIS Land Processes Distributed Active Archive Center.

In a warmer and wetter world, and with the associated increase in extreme climateclimatic events, lake outburst floods are expected to increase and pose a serious threat to the TP (Xu et al., 2024). A comprehensive understanding of the processes, causes, and mechanisms of such events is essential to improve our ability to predict and mitigate their hazard impacts. In this study, we integrate focusefocused on two notable inner inland lake outburst events: Zonag Lake on 15 September 2011 and Selin Co on 23 21 September 2023. The Donggei Cuona Lake event on 18 February 2024 iswas briefly discussed due to because of the human management ofto the lake and the relatively short duration of the outburst. The outburst processes arewere investigated by combining field surveys, remote sensing mapping, and hydrodynamic modelling. The causes and mechanisms that triggered the two events arewere also examined, which can help to develop more accurate forecasting predictive models that can better predict future extreme events by identifying specific conditions that precede outbursts.

2 Data and ~~m~~Methods~~s~~

2.1 Study area

Zonag Lake is situated in the north of Hoh Xil National Nature Reserve in Qinghai Province and the Sanjiangyuan National Park, where a large number of Tibetan antelopes are lambing, known as "Tibetan antelope delivery room" (Chen et al., 2021b). On 15 September 2011, Zonag Lake burst, forming a connected hydrological system with Kusai Lake, Hedin Noel Lake and Yanhu Lake. Zonag-Yanhu Lake basin covers a total area of ~8,564 km^2, with an extensive distribution of permafrost and periglacial landforms. The average elevation is 4600 m ~~above sea level~~ (a.s.l.)~~.~~ Based on nearby Wudaoliang meteorological station data from 1961 to 2019, the annual mean temperature is about -5.1℃ and the annual mean precipitation is 299.8 mm (Chen et al., 2021b). The region is characterized by three vegetation types: alpine meadows, ~~alpine~~ grasslands and ~~alpine~~ deserts (Liu et al., 2019).

Selin Co is the largest lake in Tibet and the second largest in the TP, with ~~an~~the area of ~2,465 km^2 in 2023. On 21 September 2023, an outburst occurred at Selin Co, resulting in flooding downstream into eastern Bange Co. The total area of Selin Co basin is ~44,437 km^2, covering 369.7 km^2 of glacier and 13,404 km^2 of permafrost (Wang et al., 2022b). Selin Co is fed by four ~~major~~main rivers: Zhajiazangbu, Boquzangbu, Alizangbu~~,~~ and Zhagenzangbu, and has several upstream exorheic lakes, including Qiagui Lake, Wuru Lake~~,~~ and Cuoe Lake ~~and so on~~. The basin is dominated by a cold, semi-arid monsoon climate, with an average temperature of around 0 °C and average annual precipitation of ~~approximately~~ ~350 mm (Tong et al., 2016).

Donggei Cuona Lake is located in the west~~ern~~ part of TP (98.55° E, 35.28° N), with ~~an~~the area of ~260 km^2 in 2023. Donggei Cuona Lake is ~~a~~an exorheic lake~~,~~ with a dam at the outlet. On 18 February ~~18,~~ 2024, a breach occurred in the left sluice chamber of Donggei Cuona Lake, causing water to flow out of~~discharge from~~ the lake. ~~Due to the short duration of the outburst and the human interventions affecting the lake, it is only briefly discussed in this paper.~~

2.~~1~~ 2 Lake ~~m~~Mapping ~~lakes~~ from optical satellite data

The lake area of the entire TP from the 1970s to 2023 was extracted using Landsat satellite images (Landsat 5/7/8/9, 30-m pixel), including 1970s, 1990, 1995, 2000, 2005, 2010, and 2013-2023, respectively (Zhang et al., 2019b). Compared to a previous study (covering 1970s-2018) (Zhang et al., 2019a), this dataset was extended to 2023, with more comprehensive records to reflect lake area changes in response to recent climate change. Specifically, the lake mapping in the 1970s was derived from the Multispectral Scanner System sensors spanning 1972-1976. The lake extent from 1990 to 2010 with five-year intervals was mapped from Landsat Thematic Mapper images. With the launch of the Landsat 8 and 9 satellites, the available ~~image and~~ data quality ~~have~~has been significantly improved, allowing ~~to map~~ the annual lake outline to be mapped~~spatial extent~~ from 2013 to 2023. Based on the MODIS-observed cloud-cover cycle, it can be found that cloud cover is significantly higher in summer (>50%) compared to autumn and winter (Zhang et al., 2017a). Additionally, lake outline ~~area~~ extraction in spring and winter are often hampered ~~affected~~ by frozen ~~lake~~ ice cover and snow~~fall~~, resulting in inaccurate lake boundaries. ~~It is also worth emphasizing that~~ Therefore, ~~the~~ October images ~~in October in autumn, particularly October of each year~~ are prioritized due to the low cloud cover and ~~the~~ relative stability of the lake area (annual maximum ~~period~~). If no images were ~~there are no~~ available ~~images~~ for October, images from ~~for~~ the previous and subsequent ~~neighboring~~ months were also~~further~~ considered.

The Normalized Difference Water Index (NDWI) using the Near Infrared and ~~GREEN~~ Green bands was used to differentiate between water and non-water features, and the optimal thresholds for each lake were

6

automatically determined using the OTSU method (Mcfeeters, 1996; Otsu, 1979). As lake boundaries are

easily confused with mountains and cloud shadows, snow and~~,~~ ice~~, and cloud shadows~~, the lake outlines

extracted in the previous step need to be visually checked and edited. Here, we manually examined each

lake outline with reference to the original Landsat image, and repaired incomplete lakes and removed to

targets that were misidentified as lakes, to produce a high-quality lake dataset.

High-resolution PlanetScope satellite images with 3-m pixel and a 1-day cycle, were used to track the

lake outburst process of Selin Co by visual interpretation, and to map~~extract~~ the ~~recent~~ area change of Selin

Co ~~of Selin Co~~ during 2022-2023 based on the NDWI index. Since June 2016, over 430+ Doves and

SuperDoves sensors from PlanetScope mission have been launched into 475-525 km sun-synchronous

orbits, circling the earth every 90 minutes (Mullen et al., 2023). It ~~can~~ provides four bands image including

red, green, blue, and NIR channels, increasing to eight bands after 2020. Although PlanetScope has a high

temporal resolution, it may not be able to completely cover the same region in one day. Therefore, the

NDWI images within 1-11 days windows were synthesized into a scene of relatively complete NDWI images,

and then a threshold of 0.02 (determined by ~~the comparing~~comparing the accuracy of extraction

boundaries based on the different thresholds) was used to produce lake boundaries in 2022-2023. In

addition, i~~I~~mages from Sentinel-2 (10-m pixel) (Yang et al., 2020) and Landsat-8 were also used to analyze

the process of Donggei Cuona Lake outburst~~s~~.

2.2 3 Lake level~~s~~ from satellite altimetry data

Sentinel-3 mission, comprising two identical polar orbiting satellites (Sentinel-3A and Sentinel-3B), was

used to track changes in the water level of Bange Co and Donggei Cuona Lake. Sentinel-3A and Sentinel-3B

were launched in February 2016 and April 2018, respectively, both equipped with a dual-frequency (Ku and

C-band) Synthetic Aperture Radar Altimeter operating in open-loop mode with a cycle period of 27 days (Xu

et al., 2021), providing high-quality observations of the lake water level. In this study, level-2 LAN_HY

products at Non Time Critical timeliness were collected for the 2016-2024 periods. The water level of the

lake with respect to the geoid (EGM2008) for the 20 Hz measurement was calculated using the following

equation (1).

$$WL = H_{alt} - R - R_{geo} - N \qquad (1)$$

where WL is lake water level, H_{alt} is the satellite altitude. R is the distance between the altimeter and the lake

surface without corrections, R_{geo} is the sum of geophysical and atmospheric corrections including the

ionosphere, wet and dry troposphere, solid earth tide and pole tide. N is the EGM2008 geoid height

referenced to the WGS84 ellipsoid. Subsequently, the 1.5 normalized median absolute deviation method

was used to remove outliers and then calculate the along-track mean.

~~The water level of Donggei Cuona Lake from 2010 to 2020 was derived from the Cryosat-2 satellite (Xu et al., 2021).~~ The area-water level linear relationship was used to obtain water levels from the 1970s to 2023

by inputting lake area (Zhang et al., 2021). The lake~~water~~ level ~~and area~~ of Selin Co is provided by Hydroweb

(Crétaux et al., 2016; 2011).

2.5 4 Climate and auxiliary data

The daily in situ precipitation ~~and temperature~~ records from the China Meteorological Administration

(https://www.cma.gov.cn) were used to the analyze long~~-~~ changes over~~s~~ several decades and precipitation

variations occurring shortly before the lake outburst event.~~short changes.~~ Meteorological data were

obtained ~~extracted~~ from the Shenzha station (30.95°N, 88.63°E) near Selin Co, Wudaoliang station (35.22°N,

93.08°E) near Zonag Lake, and Maduo station (34.92°N,98.22°E) near Donggei Cuona Lake (Figure 1). The data used covered the period from 1 January 1966 to 29 February 2024.

The monthly reanalysis dataset used in this study was derived from the fifth generation ECMWF atmospheric reanalysis (ERA5) (Hersbach et al., 2020), including geopotential heights, winds, special humidity, and other climate variables. The ERA5 data were employed in the diagnosis of climate mechanisms of the recent lake outburst events. The atmosphere was resolved using 137 levels from the surface up to a height of 80 km in the ERA5, with a grid of 31 km.

Gravity Recovery and Climate Experiment (GRACE) data was derived from Center for Space Research, University of Texas (CSR production) to estimate the change in terrestrial water storage (TWS) anomaly from 2003 to 2023 on the TP. CSR data have been widely used to estimate changes in water storage, drought and other fields because of their higher performance (Li et al., 2022; Pokhrel et al., 2021; Yi et al., 2016). In this study, ~~This study use~~thes GRACE/GRACE-FO RL06.2 Mascon Solutions ~~mascon~~was used, which is an estimation solution expressed in terms of spherical harmonic coefficients with a 0.25° grid. The M~~m~~ascon solutions with all the appropriate corrections (GAD, GIA, C20, C30, degree1) were applied in equi-angular grids.

2.~~3~~ 5 Lake outburst process from hydrodynamic model

The Hydrological Engineering Center-River Analysis System (HEC-RAS), developed by the US Corps of Engineers (https://www.hec.usace.army.mil/software/hec-ras) was used to model the outburst process, including the flow path, depth and velocity. In HEC-RAS, an implicit finite volume algorithm was used to ~~the solve~~solve 2D Saint Venant equation to two-dimensional unsteady flow, which is well suited to the outburst processes. The dam failure module of HEC-RAS was used to simulate ~~the dam~~dam failure. Difficulties of HEC-RAS in modelling erosion processes on soils due to the high discharge of Zonag Lake, only the hydrodynamic process of the Selin Co discharge was simulated.

The model inputs include the lake storage, terrain, breach width and depth, breach formation time, manning roughness coefficient, and discharge hydrograph. For the Selin Co storage, only the change in water volume in the upper layer is required due to the considerable storage capacity and the relatively small water level drop (<0.5 m). This can be determined from the area, water level, and hypsometric curve. NASADEM was used as ~~the terrain~~terrain data, as the NASADEM represents the topography in the year 2000 and the lakes on the TP experience significant expansion, the DEM values inside the interior of the lakes were replaced with elevations corresponding to the lake boundaries in 2023. The width and breach formation time of the breach was~~ ~~determined by tracking its progression using high-resolution PlanetScope imagery~~obtained from Plantscope imagery on 28 September and was set to 160 m~~. Specifically, the breach width was approximately 60 m on 23 September 2024, expanded to ~160 m by 27 September, reached ~180 m by 3 October, and finally developed to ~200 m on 8 October. Based on this progression, we estimated that the breach formation time took 18 days beginning from the initial breach on 21 September and ~~width~~the width of breach was 200 m. The depth of the breach was set to ~~0.8~~2 m, which ~~-~~is based on field measurements (Lei et al., 2024)~~due to the flat topography surrounding the breach~~. The total calculation time was set from ~~23~~21 September to 13 October 2023. ~~The breach formation time was set to 36 hours.~~The Manning roughness coefficient was set to 0.04 based on field surveys, which shows that the river channel area is covered by sparse herbaceous vegetation.~~The Manning roughness coefficient was uniformly set to 0.04.~~ As all the floodwater from Selin Co flows into Bange Co, the discharge hydrograph can be derived by calculating the increase in water volume in Bange Co after the outburst, which can be determined by area from Planetscope imagery and hypsometric curve. Due to the influence of clouds, shadow and other factors,

only the average discharge over a limited period can be obtained. ~~The continuous discharge was interpolated using the spline method. It is worth noting that the peak discharge time occurs within 0-4 days, and the peak time was assumed to be on the second day, and then the peak discharge was obtained under the constraint integrating on the average discharge over the 0-4 days.~~

To validate the reliability of the model, we implemented validation in three aspects. First, we compared the simulated water level changes in Bange Co with satellite-based measurements, as all floodwaters flowed into the lake. Second, the simulated flood path and extent were verified by comparing them with PlanetScope imagery to assess spatial consistency. Third, the simulated flood depth was validated with UAV-derived DEM measurements (the elevation differences between the riverbank and the riverbed can reflect the inundation depth of flood) of the post-breach flood channel.

2.~~4~~ 6 Climate diagnosis

To elucidate the mechanistic drivers of the recent lake outburst events, the moisture budget diagnoses and two–dimensional Takaya–Namura were employed to investigate the dynamic and thermodynamic effects contributing to precipitation change (Takaya and Nakamura, 2001), as well as the changes in atmospheric circulation, respectively. The moisture budget equations are defined as follow:

$$P' = E' - \langle \boldsymbol{V}_h \cdot \nabla_h q \rangle' - \langle \omega \partial_p q \rangle' + \delta \tag{2}$$

$$-\langle \boldsymbol{V}_h \cdot \nabla_h q \rangle' = -\langle \boldsymbol{V}_h{}' \cdot \nabla_h q \rangle - \langle \boldsymbol{V}_h \cdot \nabla_h q' \rangle - \langle \boldsymbol{V}_h' \cdot \nabla_h q' \rangle \tag{3}$$

$$-\langle \omega \partial_p q \rangle' = -\langle \omega' \partial_p \bar{q} \rangle - \langle \bar{\omega} \partial_p q' \rangle - \langle \omega' \partial_p q' \rangle \tag{4}$$

where P is precipitation, E is ~~evaporation, and~~ evaporation, V_h, q, and ω denote horizontal winds, specific humidity, and vertical pressure velocity, respectively. The variables with a prime represent monthly anomalies. $\langle \rangle$ represents a vertical integration from the surface to 100 hPa. $-\langle \boldsymbol{V}_h \cdot \nabla_h q \rangle'$ and $-\langle \omega \partial_p q \rangle'$ represent the changes in horizontal and vertical moisture advection, respectively. δ denotes the residual term. The changes in $-\langle \omega \partial_p q \rangle'$ can be divided into the thermodynamic ($-\langle \bar{\omega} \partial_p q' \rangle$), dynamic effects ($-\langle \omega' \partial_p \bar{q} \rangle$), and nonlinear component ($-\langle \omega' \partial_p q' \rangle$). The thermodynamic term reflects the contribution of moisture change, while the dynamic term represents the contribution of atmospheric circulation change.

The Takaya–Namura wave activity flux is defined as follows:

$$W = \frac{P}{2|U|} \begin{pmatrix} \bar{u}(\psi_x'^2 - \psi' \psi_{xx}') + \bar{v}(\psi_x' \psi_y' - \psi' \psi_{xy}') \\ \bar{u}(\psi_x' \psi_y' - \psi' \psi_{xy}') + \bar{v}(\psi_y'^2 - \psi' \psi_{yy}') \end{pmatrix} \tag{5}$$

where $U = (u, v)$ indicates the horizontal winds, and ψ denotes the stream function. Overbars and primes represent the climatology means and monthly disturbances, respectively.

~~**2.5 Climate and auxiliary data**~~

~~The daily in situ precipitation and temperature records from the China Meteorological Administration (https://www.cma.gov.cn) were used to the analyze long- and short-changes. Meteorological data were extracted from the Shenzha station (30.95°N, 88.63°E) near Selin Co, Wudaoliang station (35.22°N, 93.08°E) near Zonag Lake, and Maduo station (34.92°N,98.22°E) near Donggei Cuona Lake (Figure 1). The data used covered the period from 1 January 1966 to 29 February 2024.~~

~~The monthly reanalysis dataset used in this study was derived from the fifth generation ECMWF atmospheric reanalysis (ERA5) (Hersbach et al., 2020), including geopotential heights, winds, special humidity, and other climate variables. The ERA5 data were employed in the diagnosis of climate mechanisms of the recent lake outburst events. The atmosphere was resolved using 137 levels from the surface up to a height of 80 km in the ERA5, with a grid of 31 km.~~

2.7 Field surveying

The field surveying was conducted in October 2023 and August 2024 for Selin Co outburst event. During the field surveying, we examined the breach, the flood channel, and damaged roads, and inlet of Bange Co. Uncrewed aerial vehicle (UAV) was used to capture the orthophotos of flood river channel from Selin Co to Bange Co, breach, as well as road and settlements at risk. Then, high accuracy DEM was generated from UAV orthophotos using Agisoft Metashape and Context Capture software to capture the depth and extent of Selin Co flood inundation~~flood~~.

3 Results

3.1 Recent remarkable responses of lakes to climate change

From the 1970s to 2023, lakes greater than 1 km^2 on the TP experienced a significant increase in their size. The TP also experienced the formation of many new lakes. The total number and area of lakes increased from 1080 to 1537 ($\pm$42%), and from 40,124$\pm$766 to 51,928$\pm$853 km^2 ($\pm$29%), respectively, during this time period (Figure 1b-c). The shrinking trend in the lake area was observed during 1970s-1995, followed by a continuous increase in 1995-2010. Thereafter, and despite inter-annual fluctuations, the overall trend in lake area continued to increase (Figure 2). These changes mainly occurred in the endorheic TP (a large, closed basin of ~700,000 km^2), which contains more than 73% of the number and area of lakes in the region (>1 km^2).

It is important to emphasize that the expansion of lakes on the TP in 2023 is significant. The observed increase in the number and area of lakes was approximately 140 and ~1,400 km^2, respectively, which exceeds the change observed within any given year during the past 50 years (Figures 1b-c, 2). Changes of lakes in the endorheic TP are the most pronounced. The lake changes also show a synchronous increase with the TWS from 2003 to 2023, especially in the endorheic TP (Figure S1).
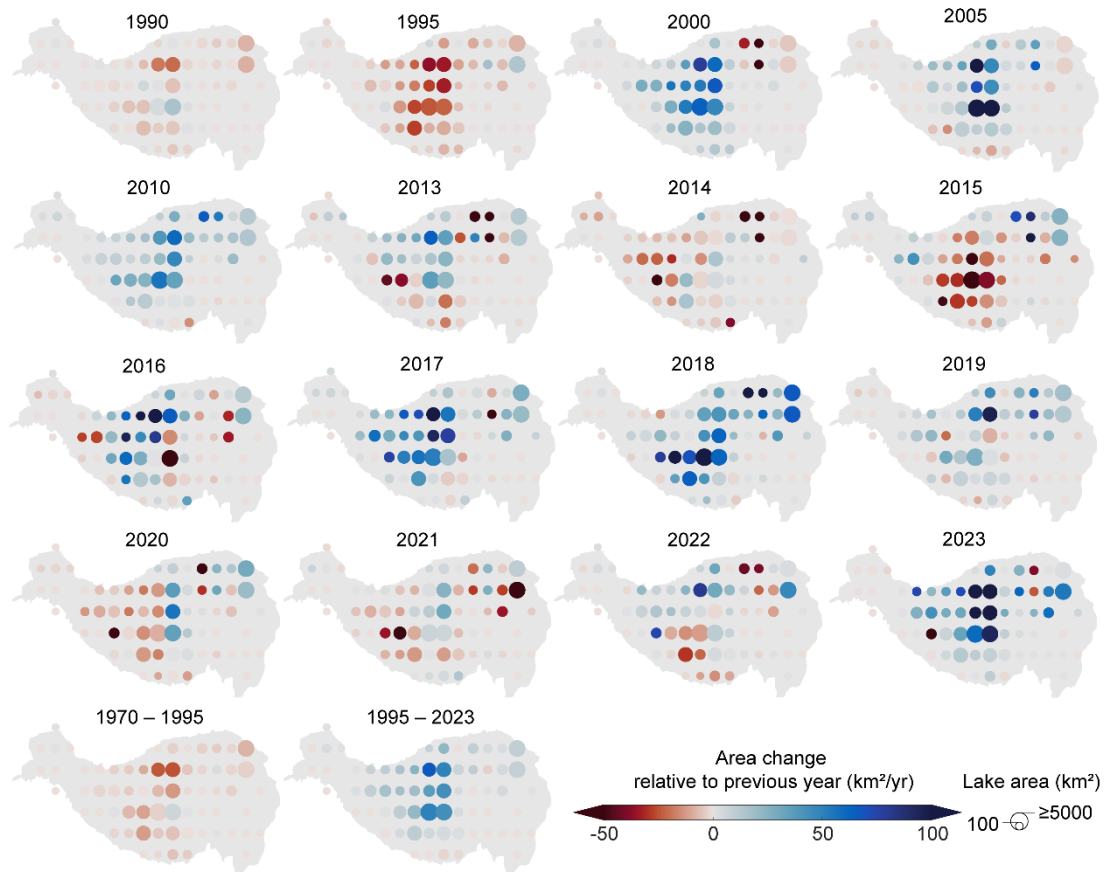
Figure 2. The spatial change of lake area on the TP. Lake area aggregated by 2×2° grid. Panels represent the average change rate in lake area relative to previous years with the available lake area data (km²/yr), divided by the time interval when a time span exists. For example, the first panel represents the changing ratio of area between 1990 and 1970. The last two panels represent the change in unit area from 1970-1995 and 1995-2023, respectively.

3.2 Processes and causes of recent lake outbursts

With the rapid expansion of lakes on the TP, signs of lake outburst become increasingly apparent. These events attract widespread attention due to their impact and the surrounding environment. For example, the outburst of Zonag Lake on 15 September 2011, the outburst of Selin Co on 24 September 2023, and dam failure of Donggei Cuona Lake on 18 February 2024 have all been devastating. Here, we focus on the outburst events in Zonag Lake and Selin Co due to their wide-ranging impacts (i.e., damage to infrastructure, ecosystems, and biodiversity) and ~~representativenes~~representativeness of the natural expansion of lakes on the TP.

3.2.1 Zonag Lake outburst event

From a long-term perspective, Zonag Lake remained relatively stable between 1975 and 2002 (with an average area of 257±1.55 km²), but then experienced an expanding trend, increasing to ~~its maximum size (~~274±1.42 km²~~)~~ on 22 August 2011 (Liu et al., 2016) (Figure 3a). On 15 September 2011, an outburst event occurred in Zonag Lake. A substantial amount of water from Zonag Lake was discharged in a short period of time due to the large width ($\sim$380 m) and depth ($\sim$27 m) of the breach and the steep gradient of the river channel (Figure S2) (Lu et al., 2021).The lake area of Zonag Lake reduced by ~107.52 km² observed by

Chinese HJ-A/B satellites satellite within 28 days (~3.84 km^2/day) (Liu et al., 2016), with water flowing downstream along the river channel into Kusai Lake. As Kusai Lake is recharged by floodwaters from Zonag Lake, it increased in size by ~38 km^2 to reach its maximum area. The water then flows into Hedin Noel Lake in the adjacent basin by forming a new channel, which then flows into Yanhu Lake (tailwater Lake). This outburst directly altered the hydrological connectivity of the drainage system, merging two basins into one. Due to the continuous inflow of water into Yanhu Lake, its size increased from 47±1.26 km^2 in 2011 to its maximum extent of 210±2.96 km^2 in 2019 (~20.37 km^2/yr).

The expansion of Zonag Lake was mainly attributed to the long-term increase in precipitation (Figure 3a), which led the lake to expand to its maximum extent, eventually causing it to overflow and burst. Extreme precipitation, defined as total annual precipitation above the 95th and 99th percentiles for the historical period from 1981 to 2010, also showed a significant increase, reaching a maximum in 2011 (Figure 4). This extreme precipitation played a key role in the lake's outburst. Additionally, two seismic events occurred prior to the breach: one on 27 July 2011 (62 km from Zonag Lake, magnitude 4.0), and another on 22 August 2011 (57 km from Zonag Lake, magnitude 3.1). These events may have weakened the geological stability of the lake dam (Liu et al., 2016). The contribution of glacier melt to Zonag Lake's expansion was relatively small. Model simulations indicate that glaciers and snow contribute around 21% to lake expansion (Wang et al., 2022a). Therefore, glacier melt plays a relatively minor role in the overall lake expansion process and outburst.
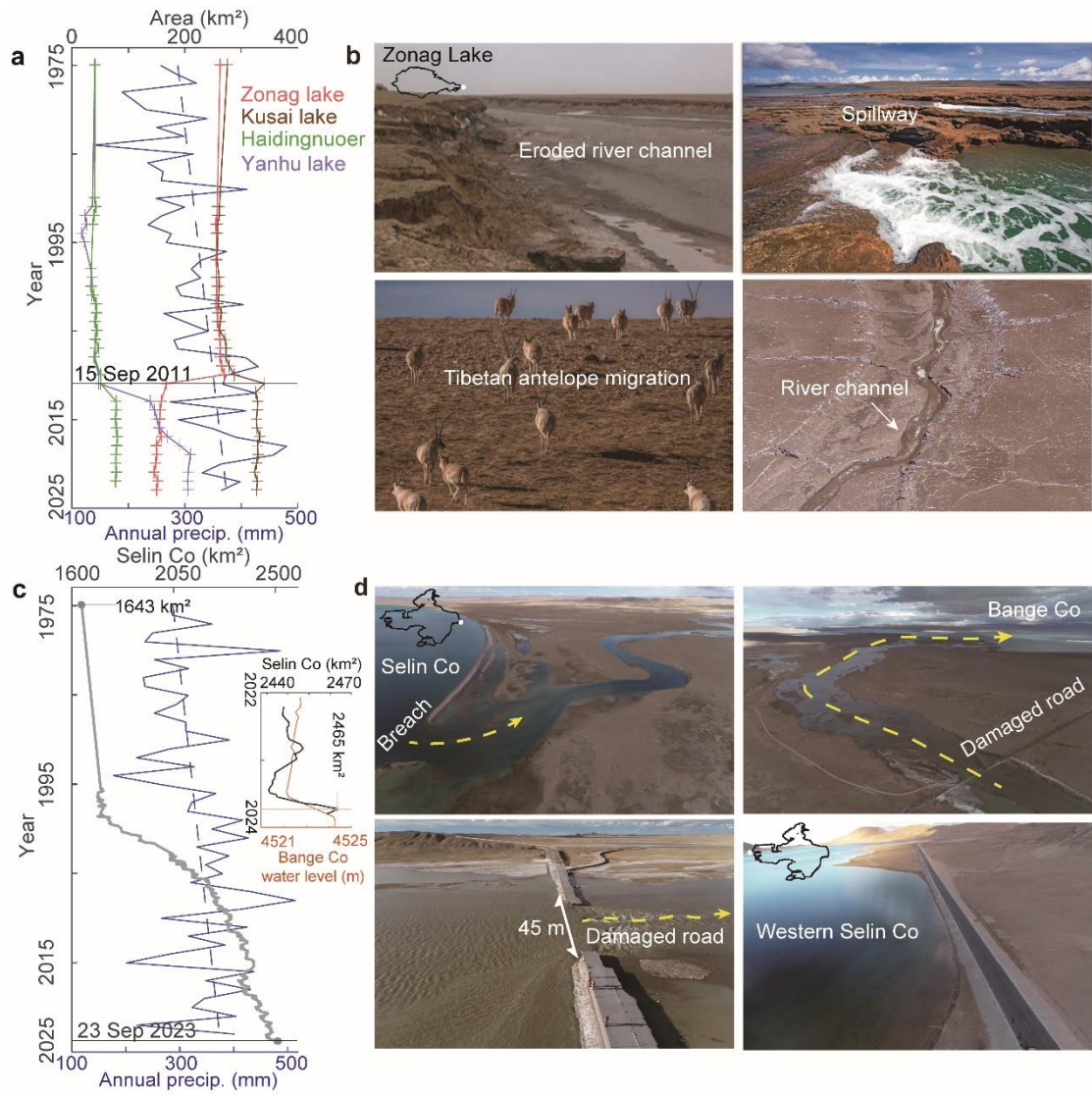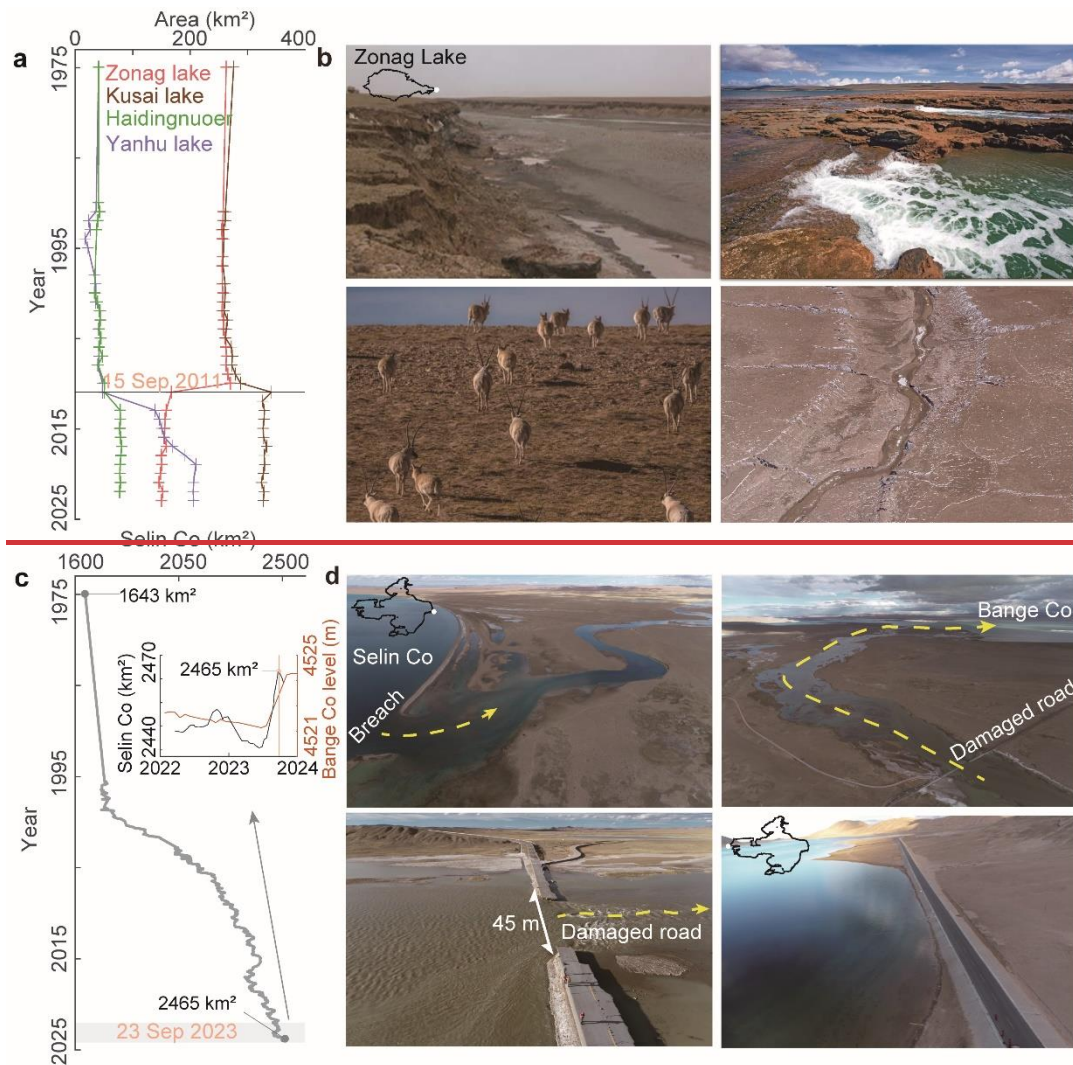
345 **Figure 3**. The changes and impacts of Zonag Lake and Selin Co. (**a**) The area change of Zonag Lake and downstream Kusai Lake, Haidingnuoer and Yanhu Lake, as well as the annual precipitation change from Wudaoliang weather stations (Blue). (**b**) The impact of Zonag Lake outburst, including the formation of new channel, soil erosion and the disruption of Tibetan antelope migration routes. (**c**) The area changes of Selin Co, as well as the annual precipitation change from Shenzha weather stations (Blue). The inset shows the rapid

350 expansion of Selin Co and Bange Co in 2022-2024. (**d**) The impact of Selin Co outburst, including formed breach, damaged road, new channel between Selin Co and adjacent Bange Co. Selin Co has also approached near the road on the south-west side (lower right panel).
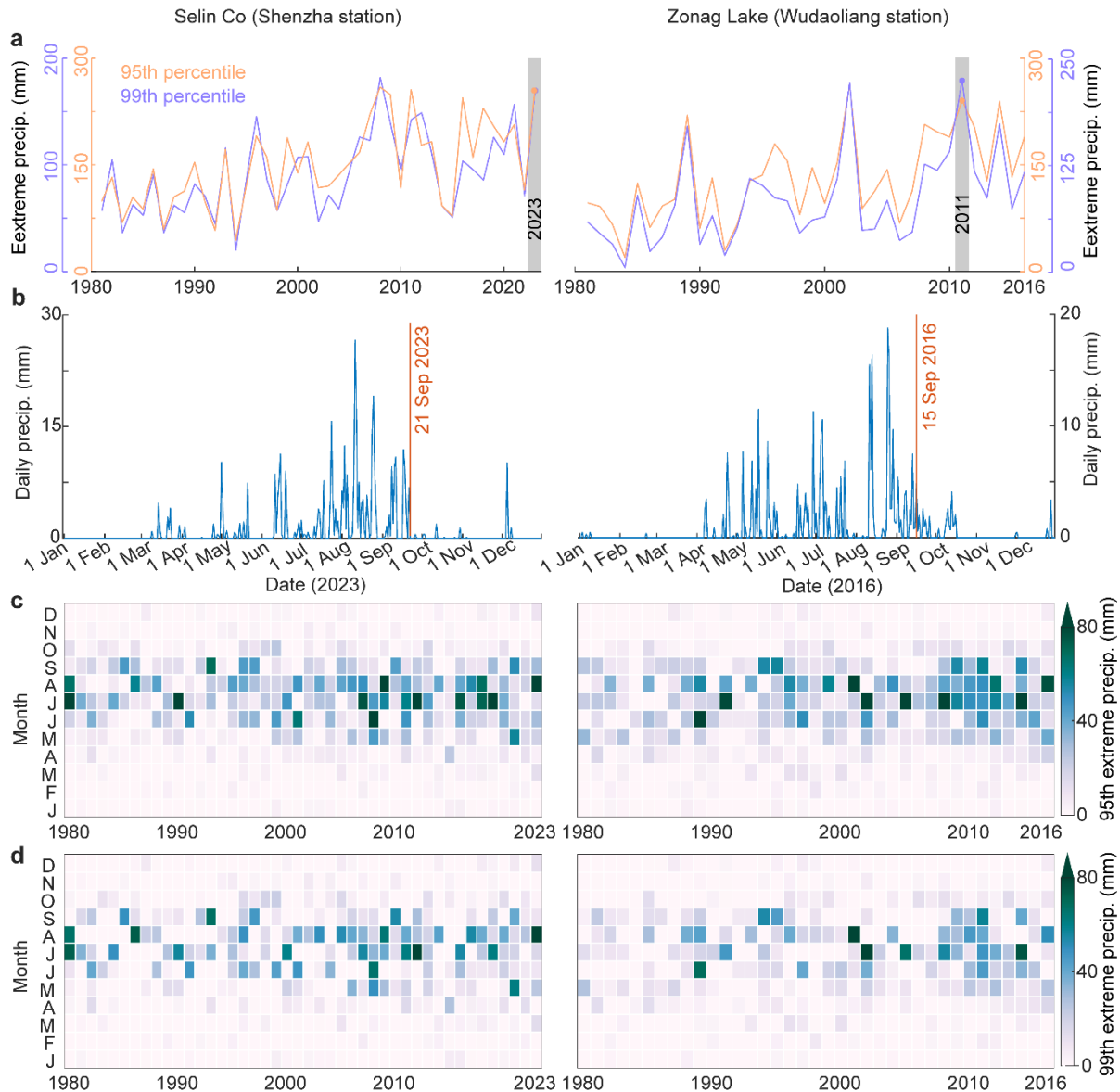
Figure 4. The change in extreme precipitation derived from Shenzha (near Selin Co) and Wudaoliang (near Zonag lake) weather stations. (**a**) Extreme precipitation (total precipitation that exceeds a 95th and 99th percentile during the historical period from 1981 to 2010) change from 1980 to 2023. (**b**) The daily change of precipitation prior to the outburst. (**c**) Monthly extreme precipitation change based on the 95th percentile from 1980 to 2023. (**d**) Monthly extreme precipitation change based on the 99th percentile from 1980 to 2023. The location of the weather station was shown in Figure 1.

3.2.2 Selin Co outburst event

Selin Co, the largest lake in Tibet and the second largest in the TP has experienced the most dramatic expansion (Figure 3b), with its area increasing by 50% from 1,643±4.52 km^2 in the 1970s to 2,465±10.82 km^2 in 2023 and its water level rising by ~15 m. Due to both long-term sustained and short-term dramatic growth, the eastern side of Selin Co experienced an outburst event on 23 September 2023, resulting in the floodwaters breaking through the S208 road and flowing into the Bange Co. Based on high-resolution satellite images, this outburst process was identified (Figure 45). Selin Co was still in normal condition on 16 September, whereas by 20 September there was already a substantial amount of water near the S208 road

15

370 indicating signs of heavy precipitation.while by 20 September water had accumulated near the S208 road, showing signs of heavy precipitation. By 23 21 September, Selin Co experienced an outburst event. , with 60 m of tThe initial breach width was found to be ~60 m by 23 September. The floodwaters initially overflowed the nearby road and with continued pressure from lake flooding, the road was subsequently broken on 24 September, causing the floodwaters to directly flow into Bange Co. On 27 September the breach widened to

375 ~160 m, and further expanded to ~200 m on 8 October. on On 13 October, the flooding was stopped by the construction of an artificial dam (Figure 5g, h). This event resulted in a water mass loss of ~0.3 Gt in 21 23 days and a water level drop of ~0.12 m for Selin Co but led to a water level rise of ~2.3 m in and an area expansion of ~18% for Bange Co (Figure 56). The maximum average discharge reached a ~287.63 m³/s on 0-4 days and then gradually decreased until 13 October (Figure 5e). Based on the average discharge line,

380 the peak occurs within 0-4 days. If the peak time occurs on the second day, the peak discharge fitted by the spline method reaches ~365.66 m³/s.
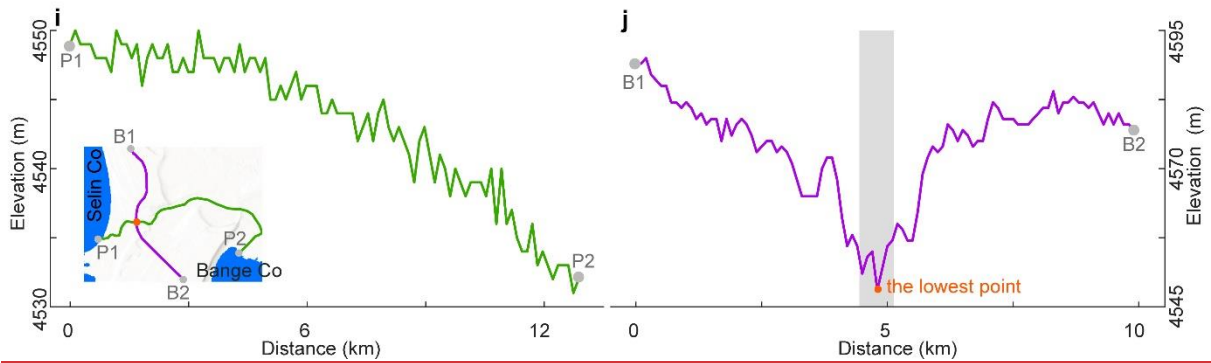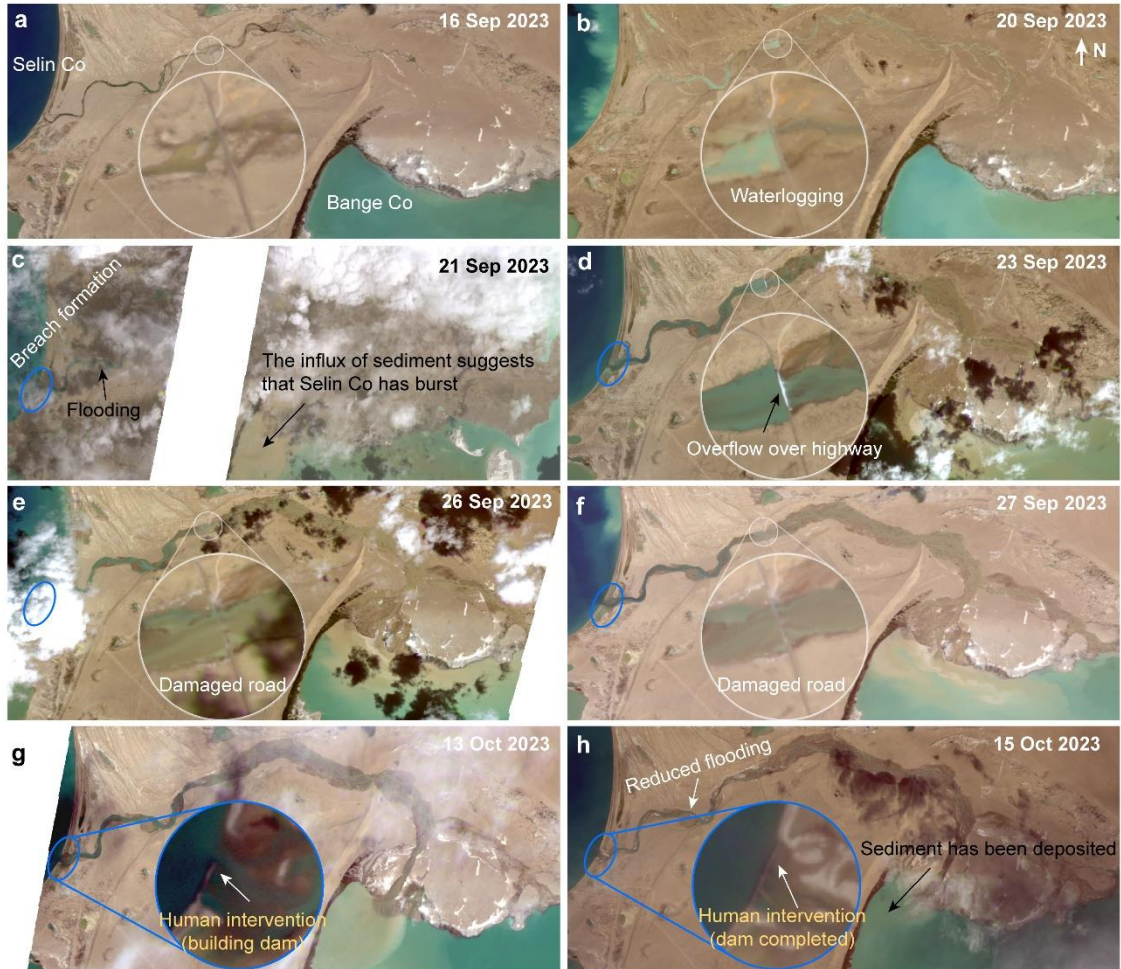
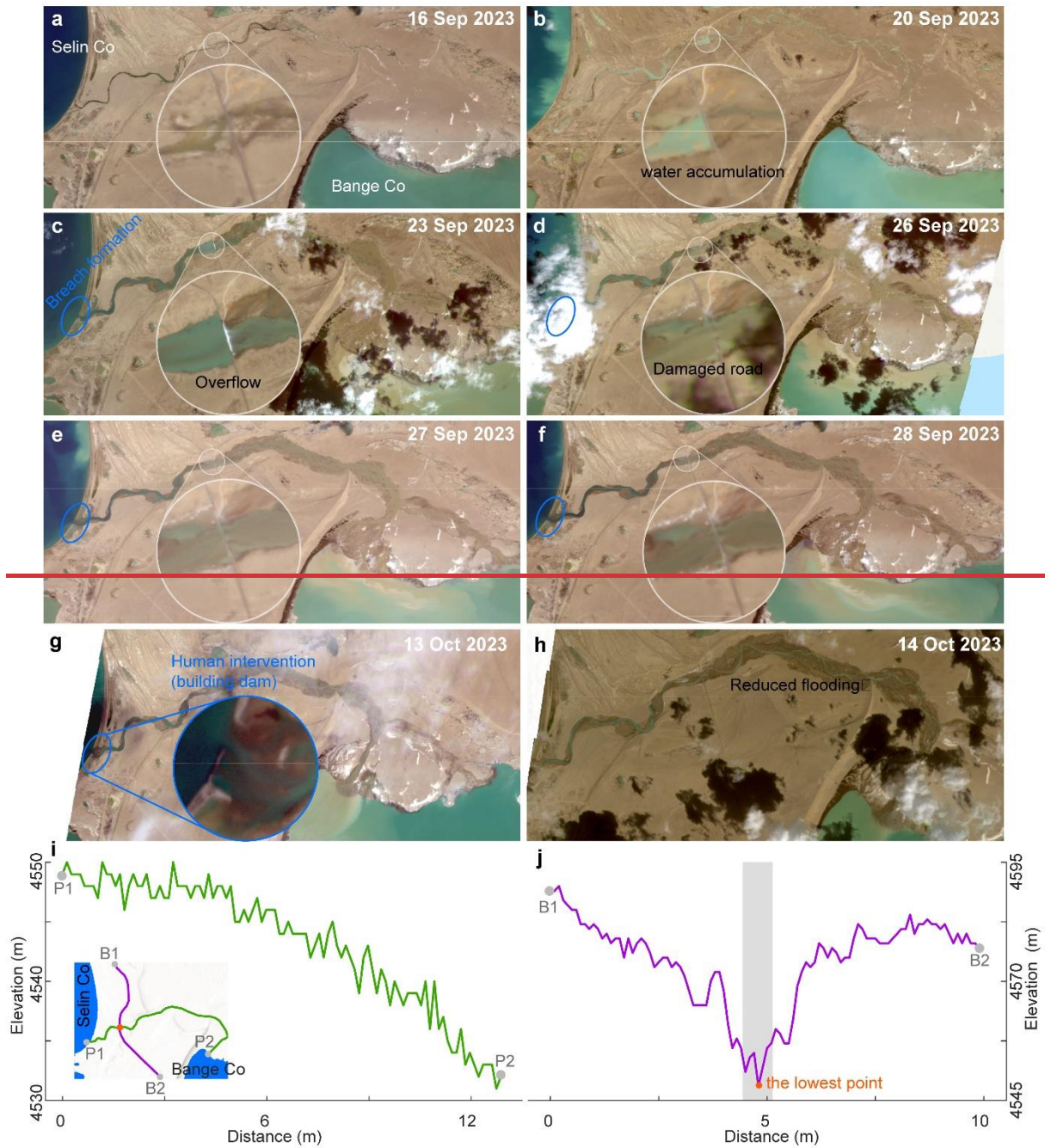**Figure ~~4~~5**. The outbrusting process of Selin Co as observed by PlantScope satellite imagery. (**a**) Selin Co remains normal. (**b**) Waterlogging due to precipitation along the roadside. (c) Sediment influx into Bange Co and flooding suggests that Selin Co has burst. (~~c~~d) Flooding from Selin Co overflowing roads. (~~d~~e) Flood from Selin Co destroys roads. (~~e,~~ **f**) Floodwater from Selin Co continues to flow into Bange Co. (**g**) Construction of a dam to block the floodwater. (**h**) Dams have been completed and flooding has been significantly reduced~~The reduced flood~~. The inset shows the damage process of the road caused by Selin Co or the newly built dam. (**i**) The elevation profile of the potential flow path between Selin Co and Bange Co before Selin Co burst. (**j**) The elevation profile of the common boundary between Selin Co and Bange basin. The inset in (**i**) shows the location of the profiles.
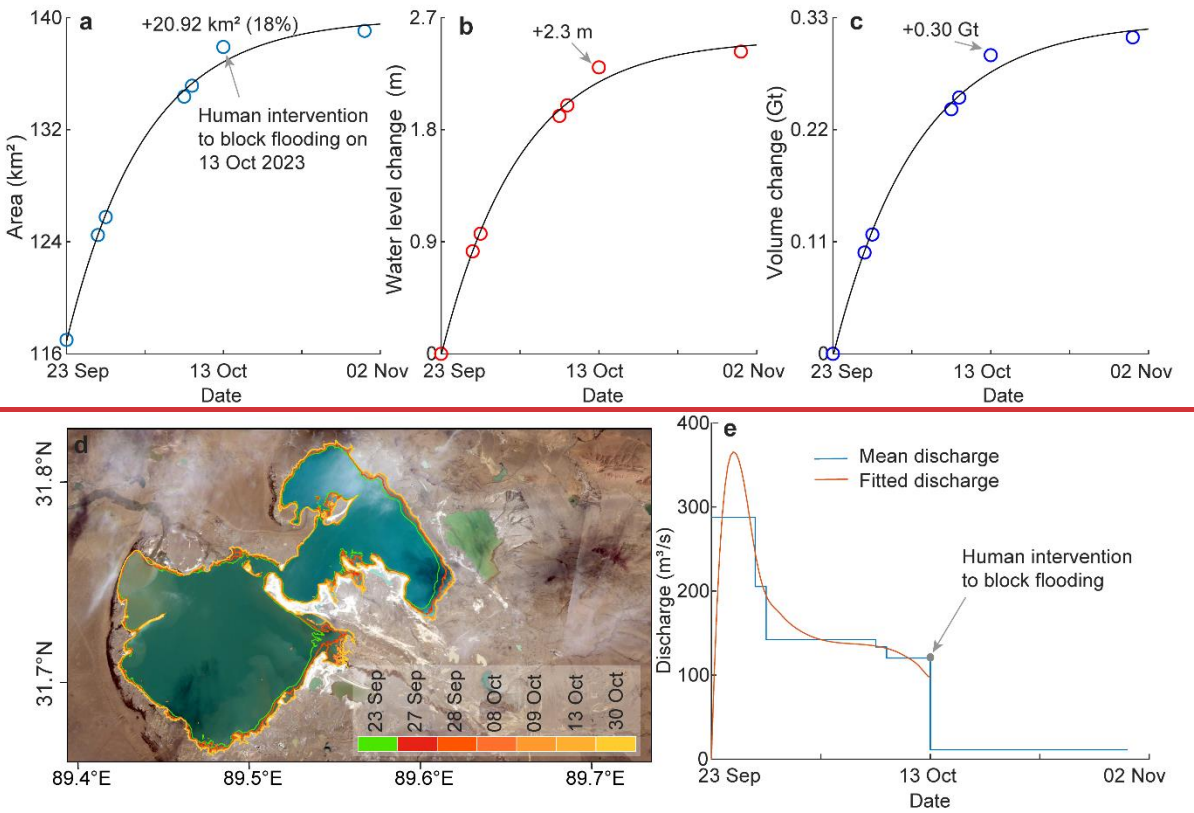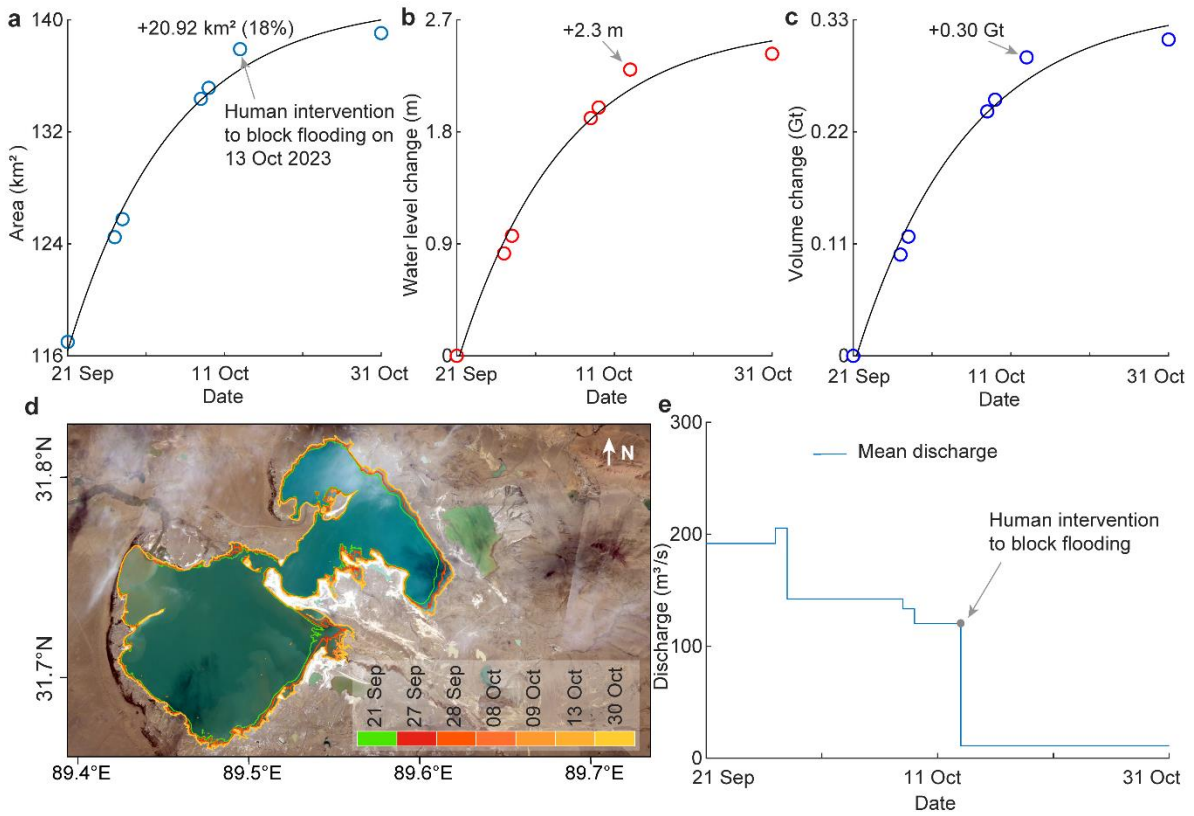
Figure 56. The water change of the downstream Bange Co after the Selin Co outburst and the discharge of the Selin Co flood. (**a**) The changes in area, (**b**) water level, (**c**) volume and (**d**) spatial extent of Bange Co after Selin Co outburst from the available PlanetScope images and hypsometric curve. (**e**) The mean

19

discharge of the Selin Co outburst flood estimated from the volume change of Bange Co. and the
continuous discharge fitted by the spline method.
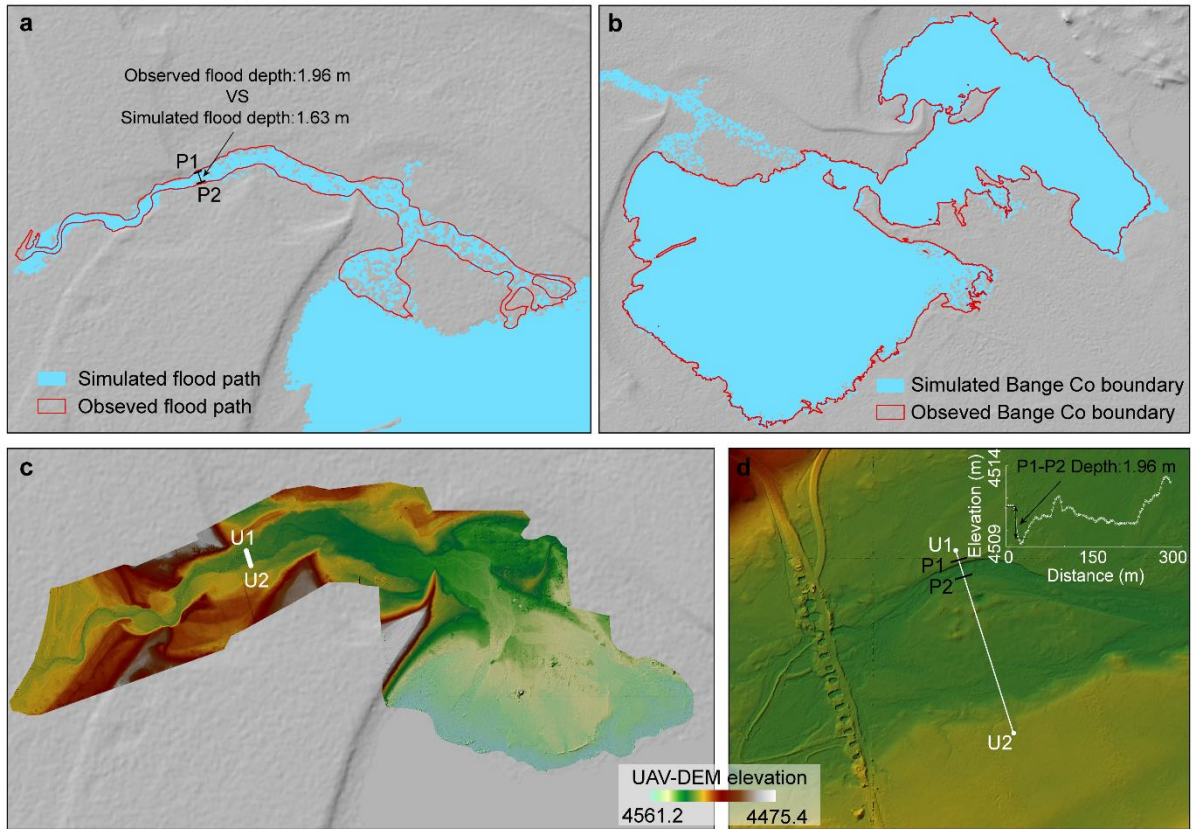
Figure 7. The validation of the Selin Co outburst flood simulation. (**a**) Comparison of the simulated flood path with PlanetScope observations of Selin Co on 13 October 2024. (**b**) Comparison of Bange Co boundary with PlanetScope observations of Selin Co on 13 October 2024. (**c**) The UAV-derived DEM of the Selin Co flood path. (**d**) The UAV-DEM near the damaged road, and the inset shows the elevation profile of the right side of the damaged road to indicate the flood inundation depth.

Based on tThe hydrodynamic simulationmodel was used to simulated the process of the Selin Co flood,. The model simulated a A water level rise of 2.23 m was observedidentified from the hydrodynamic simulation, which matches well the observed increase of 2.30 m. Additionally, the simulated flood path and extent as well as the boundary of Bange Co showed good spatial consistency with PlanetScope imagery. We also compared the simulated flood depth with UAV-derived DEM measurements of the post-breach flood channel. The model simulated flood depth at the right sideside of the damaged road was 1.63 m, while UAV measurements indicated a depth of 1.96 m, showing overall good agreement (Figure 7). the The maximum inundation depth at the damaged road reaches ~1.13 m, with a maximum flow velocity of ~1 m/s (Figure 68). Despite the modest velocity, the continuous pressure of the flood poses a significant threat, ultimately damaging the downstream road. The highest flow velocity occurs at the relatively steeply sloping inlet of Bange Co, reaching ~2.5 m/s. In addition, tThe simulation also shows that it the flood takes 1012 hours for the flood to reach the road and ~20 16 hours to reach the downstream Bange Co from the start of the breach. This suggests that even in flat areas, the impact of flooding can be significant in a short period of

time and requires the establishment of an early warning system.~~the flooding is rapid and requires the establishment of an early warning system. The simulated flood path and the changes in Bange Co water level (modelled rises of ~2.25 m), agree with remote sensing observations, confirming the reliability of the simulations.~~ The outburst of Zonag Lake has permanently altered the basin reorganization. Flood waters are discharged in a short time at very high flow rates, making effective human intervention difficult. In contrast, the discharge of the Selin Co outburst was lower, and the Selin Co outburst caused only temporary basin reorganization or a brief transition from an endorheic to an exorheic lake due to human intervention. Both lakes were endorheic lakes and burst after expanding to be ~~contained~~constrained by the terrain, emphasizing the need to monitor lakes with potential for overflow. Overflow can exacerbate erosion at the breach, thereby increasing the risk of further breaches, particularly in lakes with steep breach gradients. Zonag Lake, with its large topographic gradient at the breach and large breach, had an extremely high discharge, averaging ~~2,191~~2,238 m³/s in 28 days. In contrast, Selin Co, despite its large storage capacity, had an average discharge of ~~~170~~154.2550 m³/s in ~~21~~23 days due to its flat terrain (Figure 6e). However, even at lower velocities, flooding could threaten roads within ~~12~~10 hours, severely limiting emergency response.
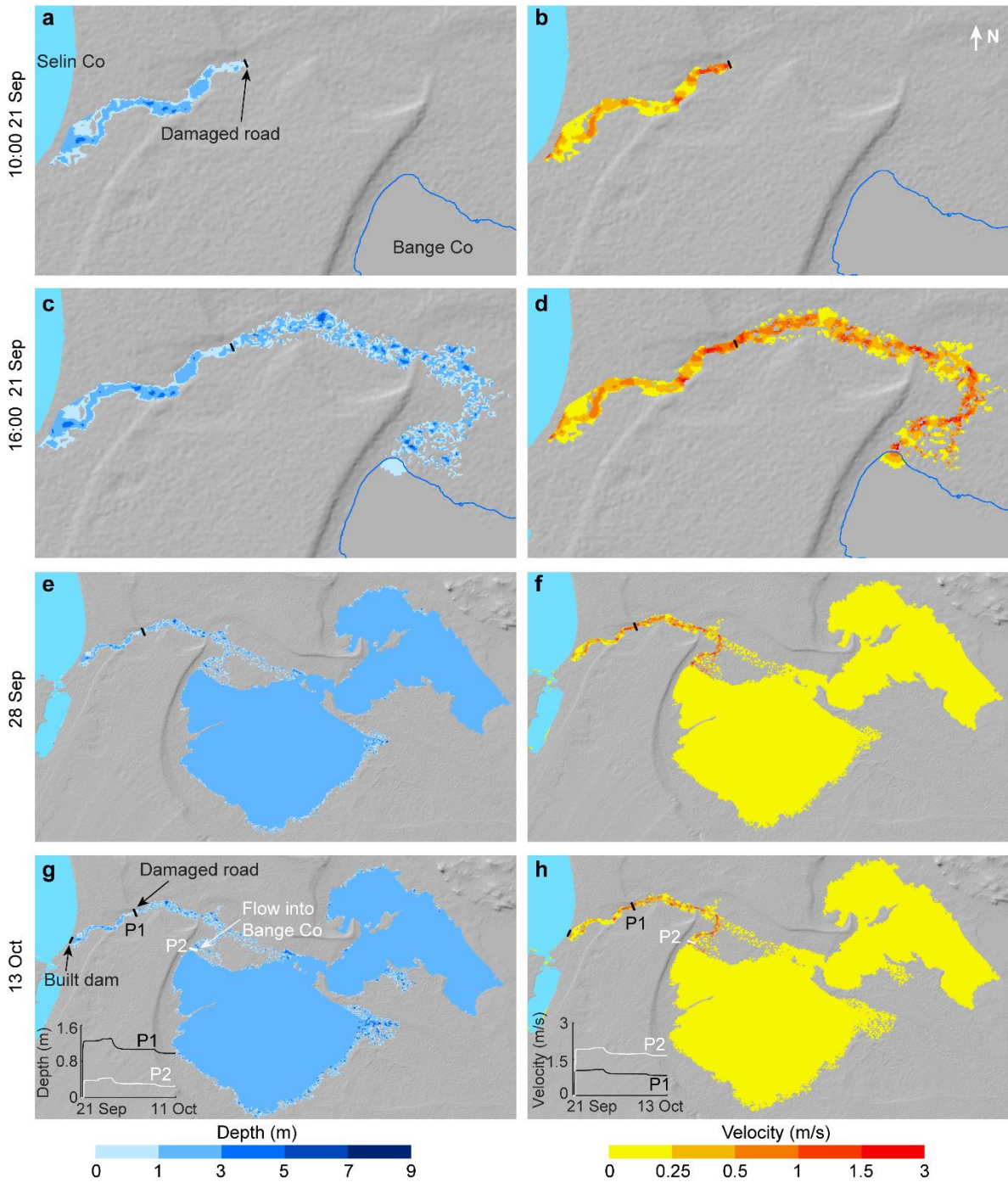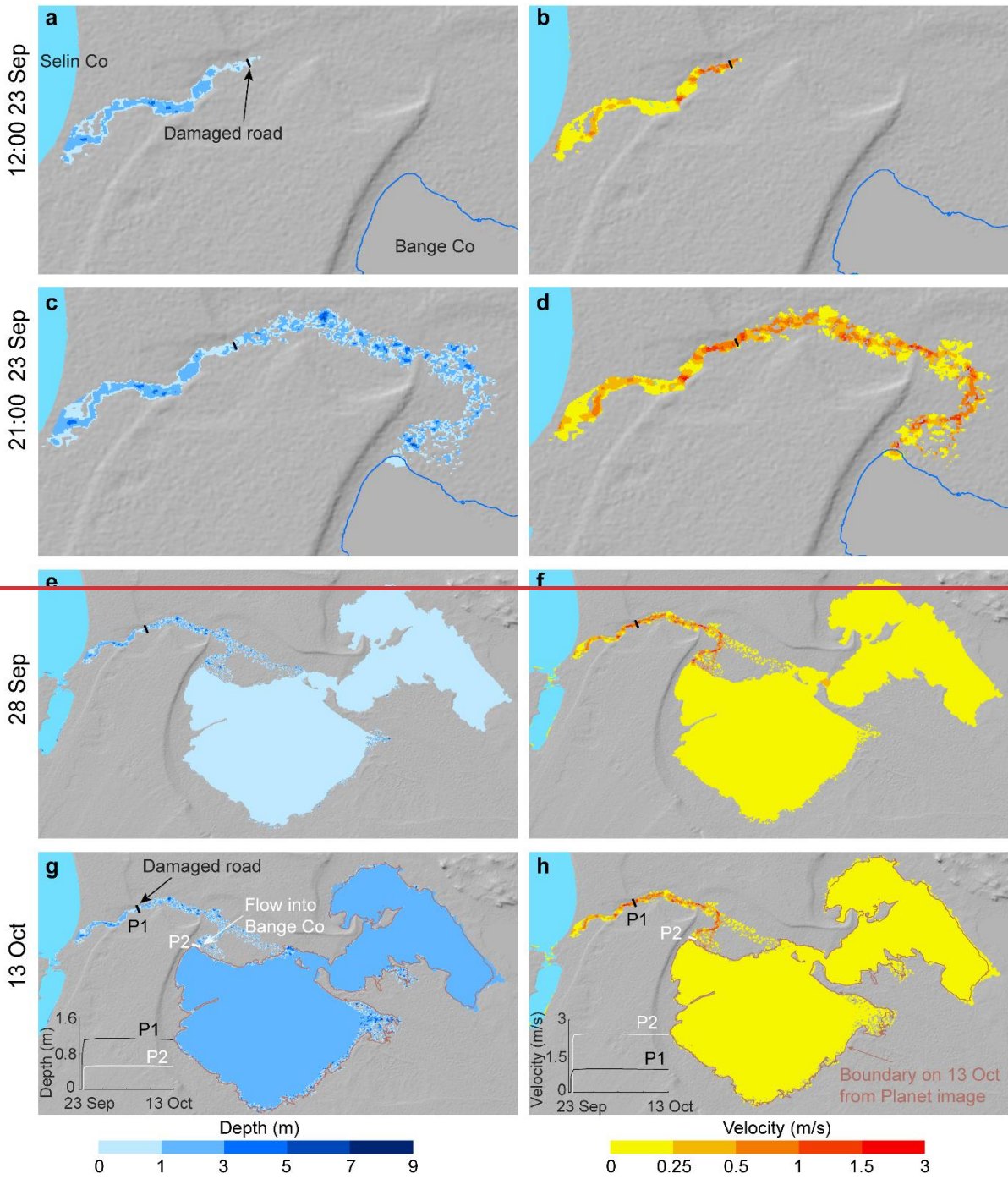
Figure ~~6~~8. The outburst processes of the Selin Co outburst flood, including modelling of the discharge path, depth, and flow velocity. (**a, b**) The flood reaches the road. (**c, d**) The flood flows into the downstream Bange Co. (**e, f**) Flood ~~condicitions~~simulation on ~~27~~ 28 September 2023. (**g, h**) The flood was stopped by human intervention by building a dam at the breach. The Inset shows the changes in depth and velocity near the damaged road and the mouth of the downstream Bange Co.

The expansion of Selin Co was similarly driven by a long-term increase in precipitation (Figure 3c), causing the lake to reach its maximum extent before overflowing and bursting (Figure 5i, j). Extreme ~~precipitation,~~precipitation increased as well, peaking in 2023 (Figure 4a), which also contributed to the lake's outburst. The contribution of glacier melt to Selin Co's expansion was relatively minor. DEMs derived from

KH-9 and CoSSC-TanDEM-X data estimate glacier contributions to lake expansion at approximately 3.5% to 16.3% (Chen et al., 2021a). Similarly, degree-day model simulations from 1976 to 2013 suggest a contribution of about 10% (Tong et al., 2016).

455   The expansion of Zonag Lake and Selin Co was mainly attributed to the long-term increase in precipitation (Figure 7), which resulted in the lakes expanding to their maximum extent and subsequently overflowing and bursting. In addition, extreme precipitation (defined as total annual precipitation above the 95th and 99th percentiles for the historical period from 1981 to 2010) also showed an increase, reaching a maximum in 2011 in Zonag Lake and in 2023 in Selin Co, which also played a significant role in the lake
460 outbursts. In addition, seismic events prior to the breach may have weakened the geological stability of the dam (Liu et al., 2016).(Chen et al., 2021a; Tong et al., 2016; Wang et al., 2022a)
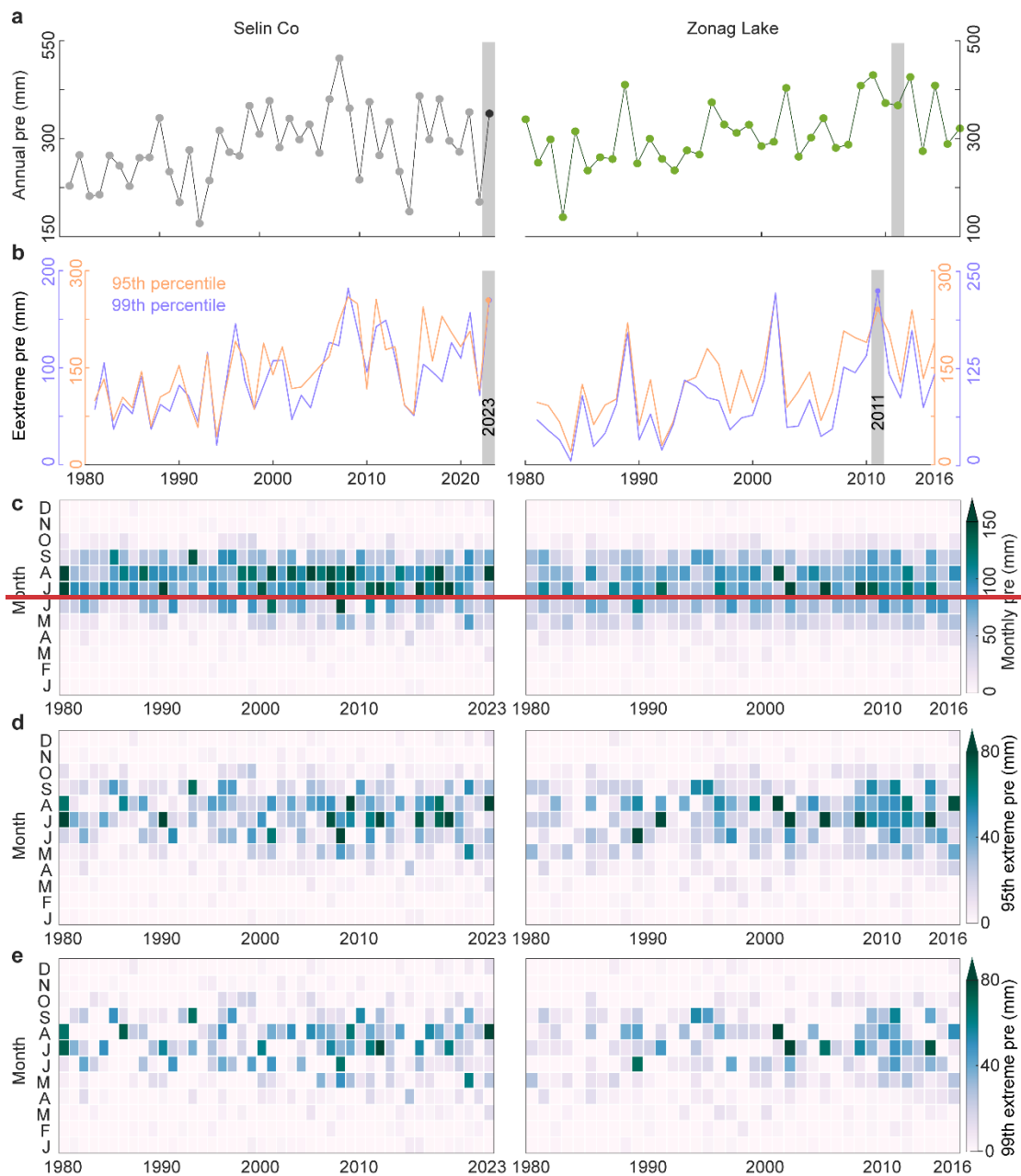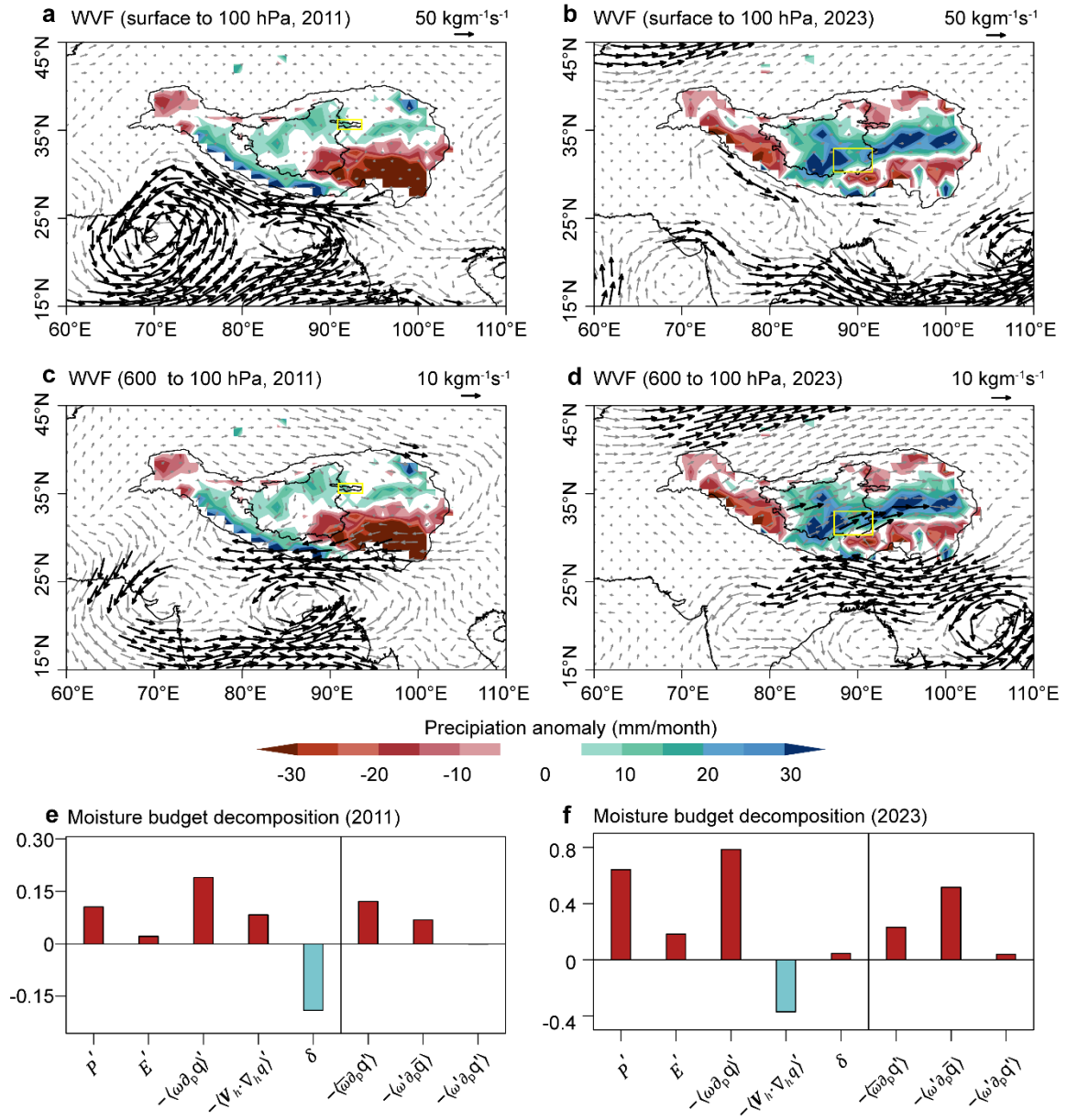

Figure 7. The change in annual and extreme precipitation derived from Shenzha (near Selin Co) and

24

3.3 Climate Mechanisms of recent lake outbursts

The Zonag Lake and Selin Co outbursts were triggered by the continuous expansion of the lakes due to a long-term increase in precipitation, as well as continuous heavy or extreme precipitation prior to the outbursts. (Figure 4), underscores the necessity of investigating the climate mechanisms. Understanding the driving mechanisms of heavy precipitation is critical, not only to help explain the observed rainfall phenomena, but also to predict future flood risks under changing climate conditions. However, the atmospheric mechanisms behind the increased precipitation during these two outburst events remain unclear. Here, we explore the contribution of each term of the moisture budget (equations (2)-(4)) to the increased precipitation within Zonag lake basin in 2011 and Selin Co basin in 2023, respectively, thus providing a more comprehensive understanding of the factors leading to these outburst events.

The increased precipitation observed in these two recent lake outburst events was primarily attributed to the reinforced influence of vertical moisture advection (Figure 9). However, the contributions of thermodynamic ($-\langle\overline{\omega}\partial_p q'\rangle$) and dynamic effects ($-\langle\omega'\partial_p\overline{q}\rangle$) exhibited notable disparities between the two occurrences. The thermodynamic effect dominated the increased precipitation in Zonag Lake basin, highlighting the important role of the warming-induced increases in the atmospheric moisture content (Figures 9e, Figure S9). In contrast, the dynamic effect contributed mostly to the increased precipitation in Selin Co basin during 2023, indicating the prevailing influence of vertical motion resulted from changes in atmospheric circulation (Figures 9f, Figure S10). It is noteworthy that horizontal moisture advection played a different role in the precipitation variations during the Zonag Lake and Selin Co outbursts, with a beneficial effect on the Zonag Lake event and a detrimental influence on the Selin Co event. This is evidenced by the anomalous moisture transport. In 2011, the enhanced southward moisture on the northern TP resulted in more moisture input in Zonag Lake basin. In 2023, the prevalence of anomalous clockwise moisture flux circulation over the southern TP led to the northward transport of moisture towards the southern area of Selin Co, consequently triggering ascending motion. Simultaneously, the intensified westerlies over Selin Co gave rise to a net outflow of moisture, resulting in negative horizontal moisture advection.
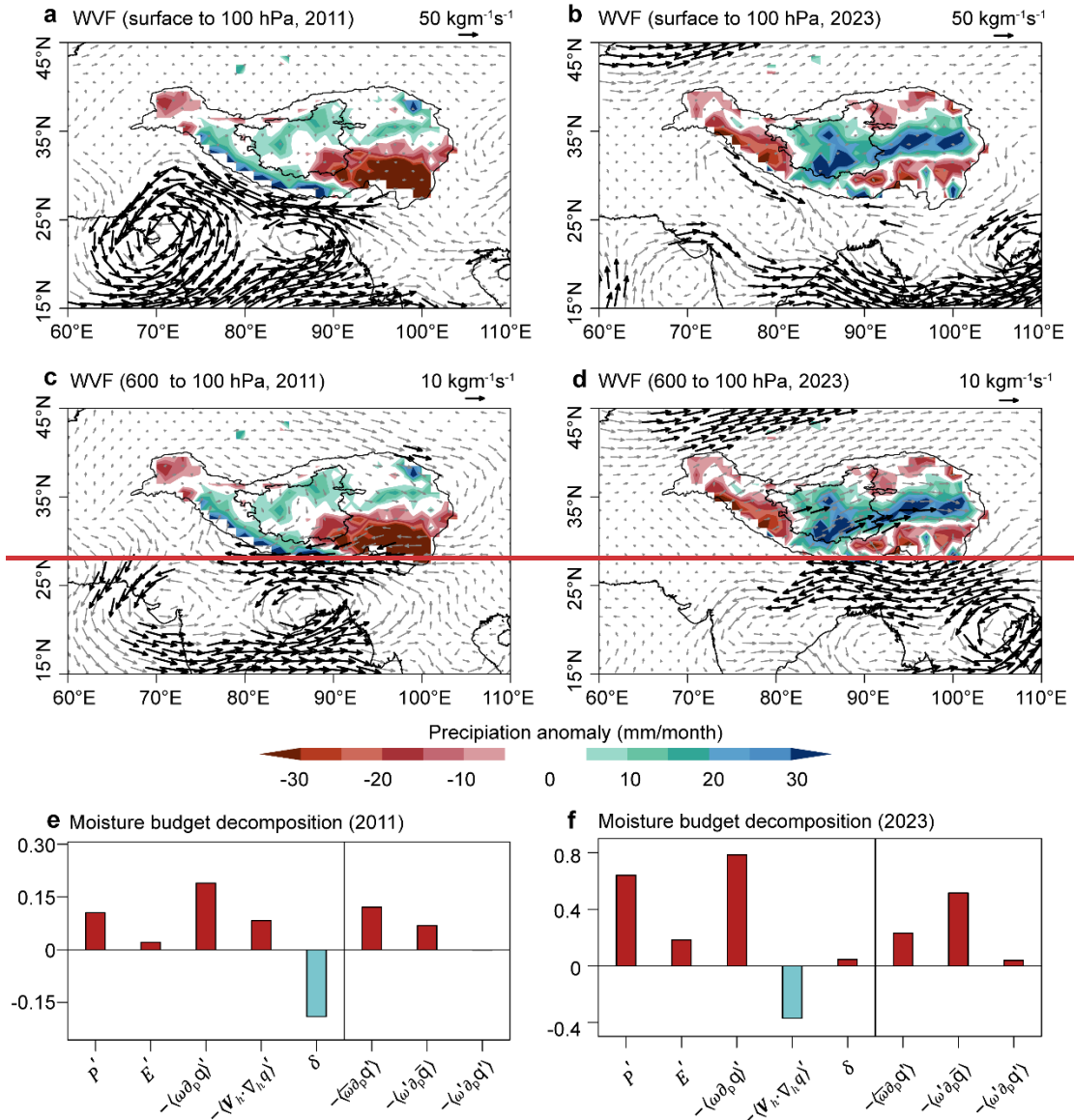
a WVF (surface to 100 hPa, 2011) 50 kgm⁻¹s⁻¹

b WVF (surface to 100 hPa, 2023) 50 kgm⁻¹s⁻¹

c WVF (600 to 100 hPa, 2011) 10 kgm⁻¹s⁻¹

d WVF (600 to 100 hPa, 2023) 10 kgm⁻¹s⁻¹

Precipiation anomaly (mm/month)

-30   -20   -10   0   10   20   30

e Moisture budget decomposition (2011)

f Moisture budget decomposition (2023)

P' E' $-\langle\omega\partial_p q\rangle'$ $-\langle V_h\cdot\nabla_h q\rangle'$ δ $-\langle\bar\omega\partial_p q'\rangle$ $-\langle\omega'\partial_p\bar q\rangle$ $-\langle\omega'\partial_p q'\rangle$

Figure ~~8~~9. The atmospheric mechanism of precipitation-induced events in Zonag Lake and Selin Co. (**a, b, c, d**) Composite maps of anomalous vertically integrated moisture flux based on ERA5 data (WVF; integrated from surface to 100 hPa and from 600 to 100 hPa; vector; $kgm^{-1}s^{-1}$) in Zonag Lake basin during 2011 and Selin Co basin during 2023. The shading indicates precipitation anomalies. The black vectors indicate WVF exceeds the reference value. The reference climate state was selected as the average from 1981 to 2010. The yellow boxes represent the location of the Zonag Lake and Selin Co, respectively. (**e, f**) The contribution of each term (precipitation (P'), Evaporation (E'), the change in vertical ($-\langle \omega \partial_p q \rangle'$) and horizontal moisture advections ($-\langle V_h \cdot \nabla_h q \rangle'$), residual term ($\delta$), thermodynamic $-\langle \bar{\omega} \, \partial_p q' \rangle$, dynamic ($-\langle \omega' \, \partial_p \bar{q} \rangle$), and the nonlinear effects ($-\langle \omega' \, \partial_p q' \rangle$)) of moisture budget components (mm/day) to precipitation changes averaged over the Zonag Lake and Selin Co basins.
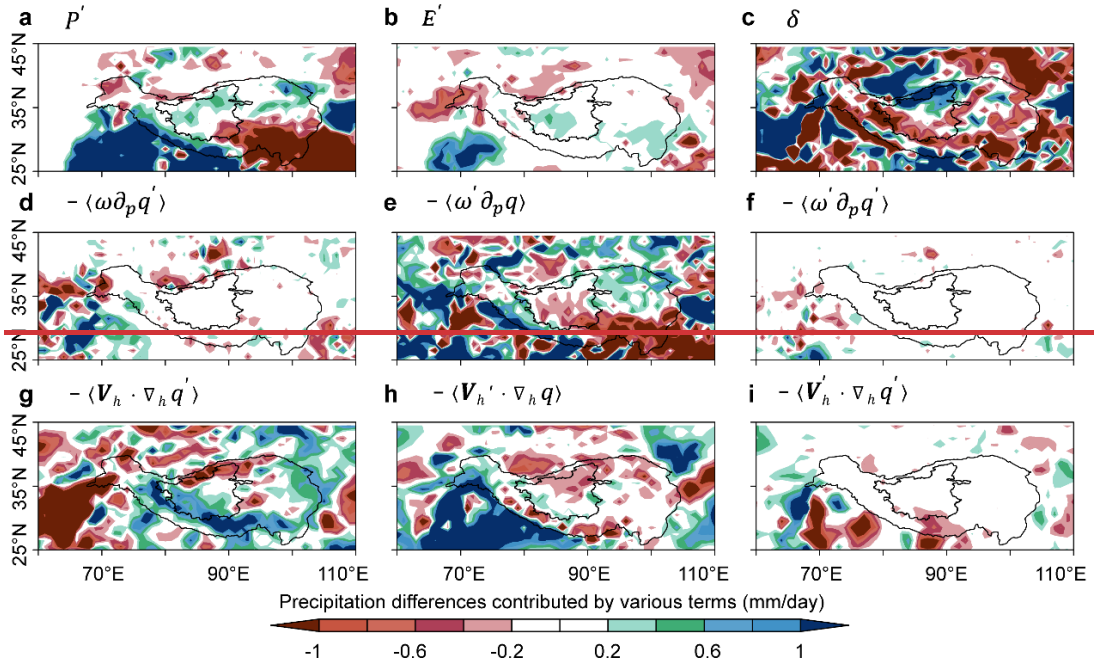
Figure 9. The moisture budget components (mm/day) in 2011. (**a**) precipitation (P'). (**b**) Evaporation (E'). The horizontal moisture advection induced by (**d**) thermodynamic $-\langle\bar{\omega}\,\partial_{\bar{p}}q'\rangle$, (**e**) dynamic $-\langle\omega'\,\partial_{\bar{p}}\bar{q}\rangle$, the nonlinear effects (**f**) $-\langle\omega'\,\partial_{\bar{p}}q'\rangle$ and (**i**) $-\langle V_h'\cdot\nabla_h q'\rangle$, (**c**) residual term, and (**g**) moisture changes $-\langle V_h\cdot\nabla_h q'\rangle$, (**h**) anomalous winds $-\langle V_h'\cdot\nabla_h q\rangle$ (**i**) $-\langle V_h'\cdot\nabla_h q'\rangle$.
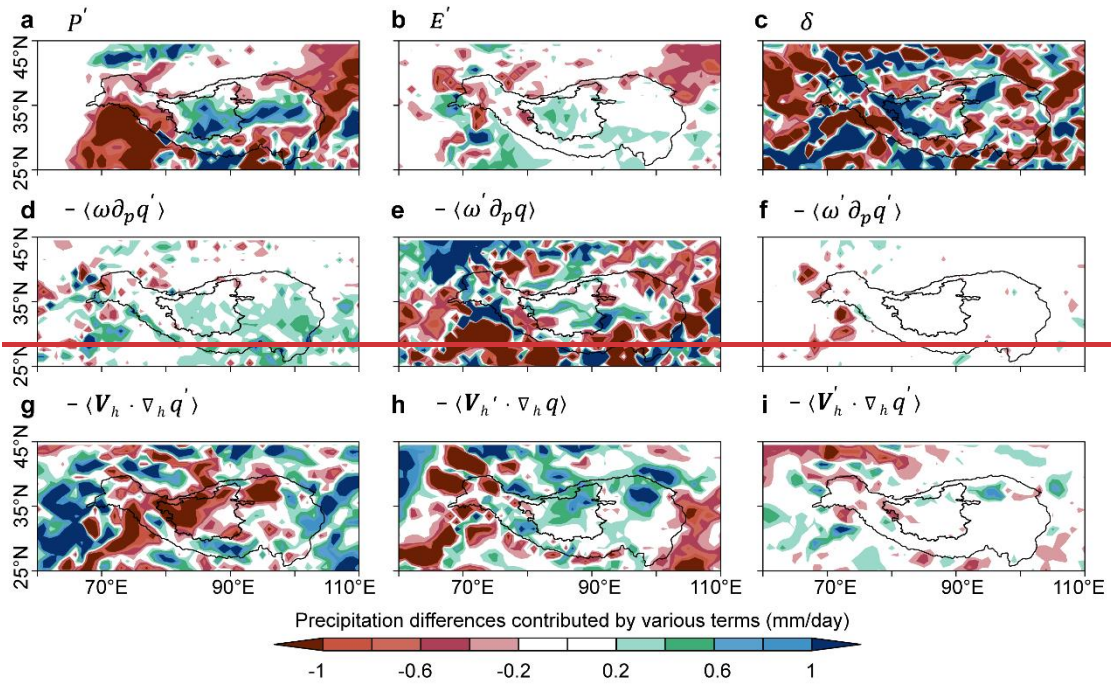
Figure 10. The moisture budget components (mm/day) in 2023. (**a**) precipitation (P'). (**b**) Evaporation (E'). The horizontal moisture advection induced by (**d**) thermodynamic $-\langle\bar{\omega}\,\partial_{\bar{p}}q'\rangle$, (**e**) dynamic $-\langle\omega'\,\partial_{\bar{p}}\bar{q}\rangle$, the nonlinear effects (**f**) $-\langle\omega'\,\partial_{\bar{p}}q'\rangle$ and (i) $-\langle V_h'\cdot\nabla_h q'\rangle$, (**c**) residual term, and (**g**) moisture changes $-\langle V_h\cdot\nabla_h q'\rangle$, (**h**) anomalous winds $-\langle V_h'\cdot\nabla_h q\rangle$.

Changes in regional atmospheric circulation play a pivotal role in modulating moisture transport and

precipitation variations on the TP. Hence, we extended our inquiry to encompass the investigation of large-scale atmospheric circulation anomalies and the propagation of corresponding wave activity fluxes during the Zonag Lake and Selin Co outbursts (Figures 1110-1211). A wave train emanating from the North Atlantic to Eurasia is evident in both 2011 and 2023; however, the propagation paths and strengths of these two wave trains exhibited notable disparities, with the wave train in 2011 being relatively flat and the wave train in 2023 being curved. In particular, the intensified wave activity fluxes over the East European Plain facilitated downstream wave propagation, leading to the establishment of negative potential geopotential height anomalies over Central Asia and positive potential geopotential height anomalies over the southern TP in 2023. This atmospheric circulation pattern was closely related to the moisture transport in the Selin Co basin, highlighting the important role of atmospheric circulation changes in lake outburst.
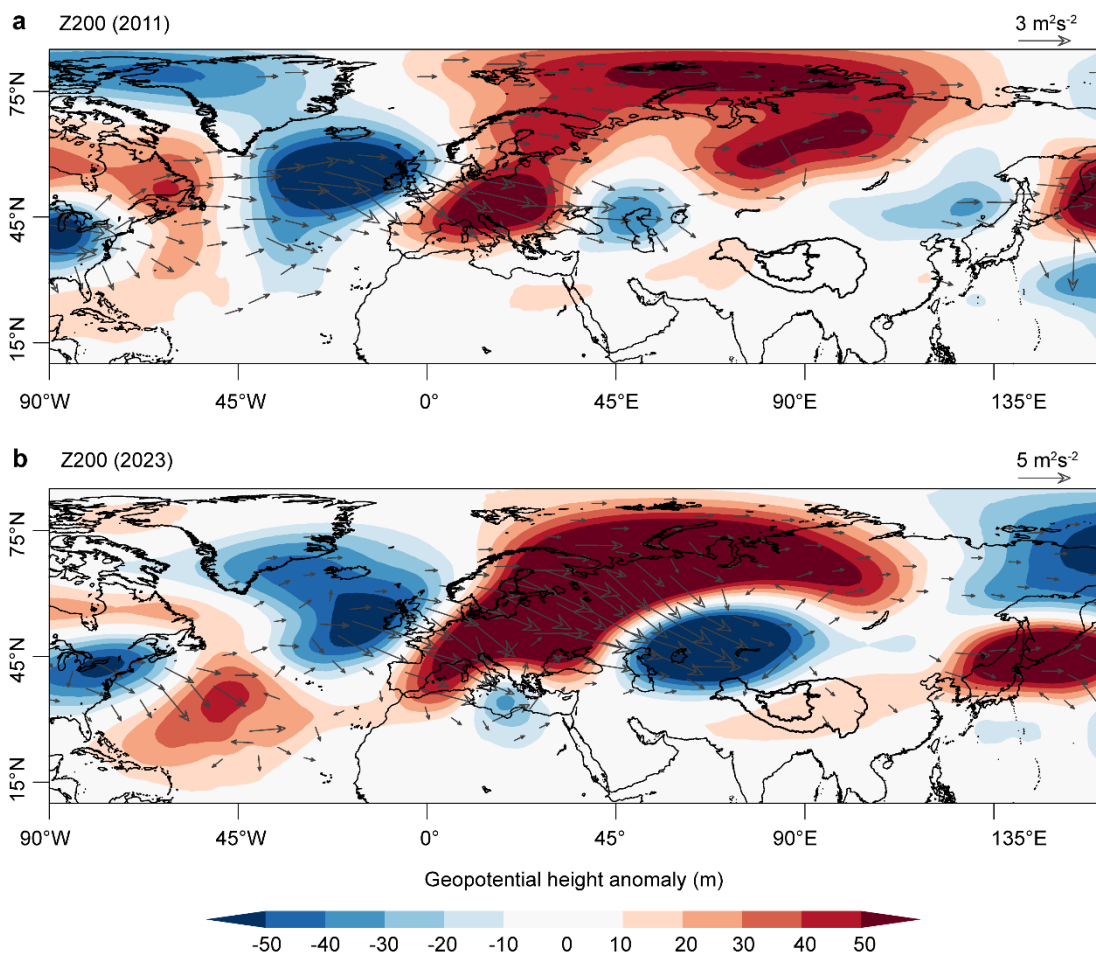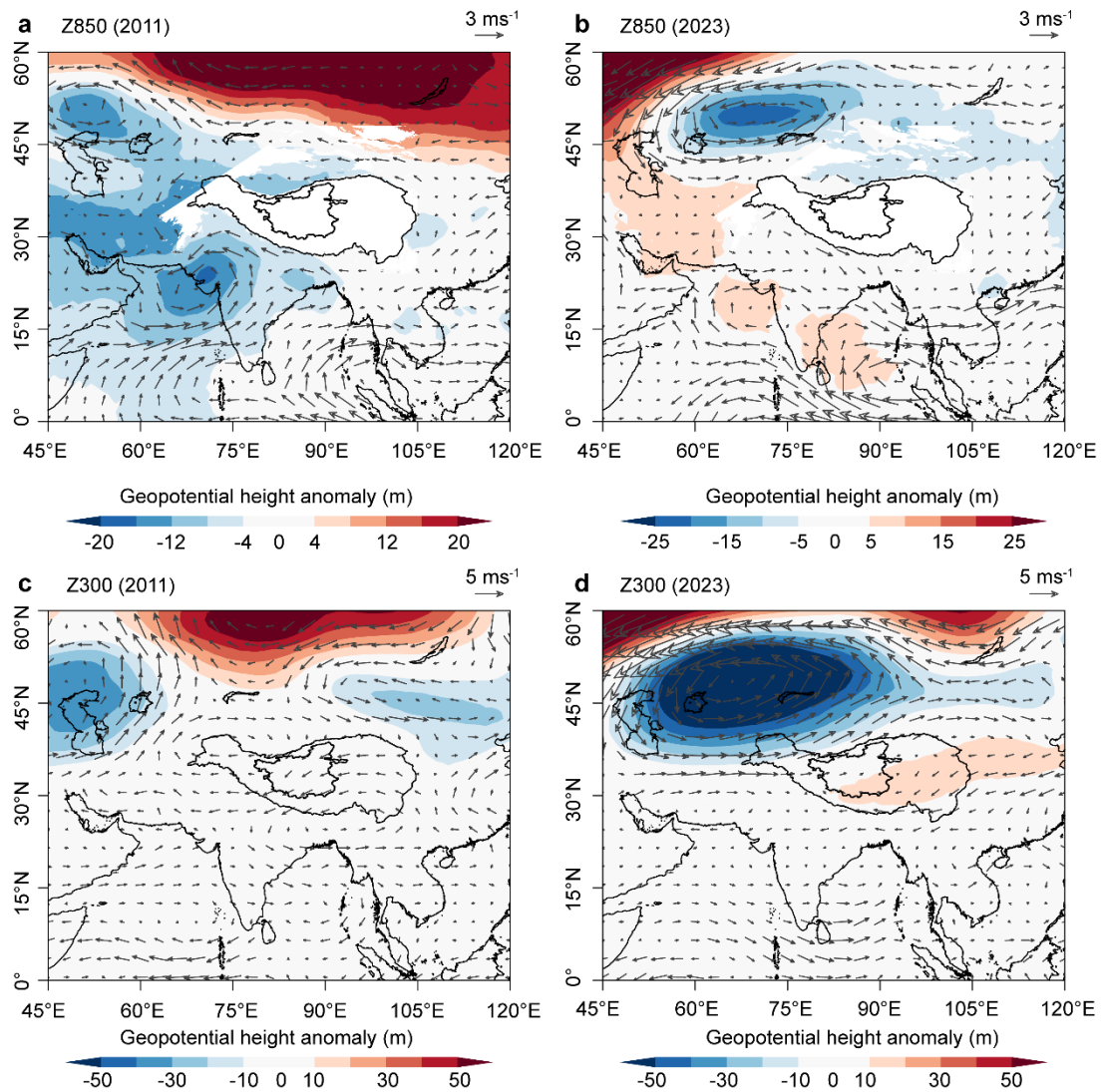

Figure 1110. The spatial distribution of geopotential height anomaly (m) at 200 hPa in 2011 (**a**) and 2023 (**b**), resepctively. The arrows indicate wave activity fluxes. The reference climate state was selected as the average from 1981 to 2010.

Figure 1~~1~~2. The spatial distribution of geopotential height anomaly (m) at 850 and 300 hPa, in 2011 and 2023, respectively. The arrows indicate wind vectors.

4 Discussion

4.1 Climate impact~~s~~ on recent lake outburst~~s~~

Lake outbursts are mainly caused by the long-term, and sustained expansion of ~~lake~~ surface area driven primarily by increased precipitation, as well as short-term dramatic expansion due to extreme precipitation events. The decadal increase in precipitation on the TP can be attributed to the external forcing, Pacific Decadal Oscillation (PDO), and Atlantic Multidecadal Oscillation (AMO) (Liu et al., 2021; 2023). For example, the combined influence of external forcing and the PDO could result in an anomalous cyclone over the ITP and a weakened East Asian westerly jet, subsequently contributing to the decadal increase in precipitation in the Inner-ITP (Liu et al., 2023). A positive phase of the AMO may lead to a northward shift and weakening of the subtropical westerly jet stream, which in turn affects moisture transport and results in changes in precipitation patterns (Liu et al., 2021; Sun et al., 2020). While the extreme precipitation events during the summer on the TP may be linked to the El Niño–Southern Oscillation (ENSO) (Figure S3) (Lei et al., 2019). The increased precipitation for the two events investigated in this study was largely attributed to enhanced vertical moisture advection, with distinct differences in the dominance of thermodynamic and dynamic effects.

30

Specifically, the thermodynamic effects played a more important role in the Zonag Lake outburst event, whereas dynamic effects predominated during the Selin Co outburst. It is evident that the increased precipitation resulting from climate warming and regional atmospheric circulation alternations has intensified lake expansion on the TP. Nonetheless, additional inquiry is warranted to reveal the distinct contributions of thermodynamic and dynamic effects to extreme lake expansion in various regions of the TP, particularly in understanding the mechanistic drivers of lake outburst events. This will be critical for understanding the response of the TP to climate warming.
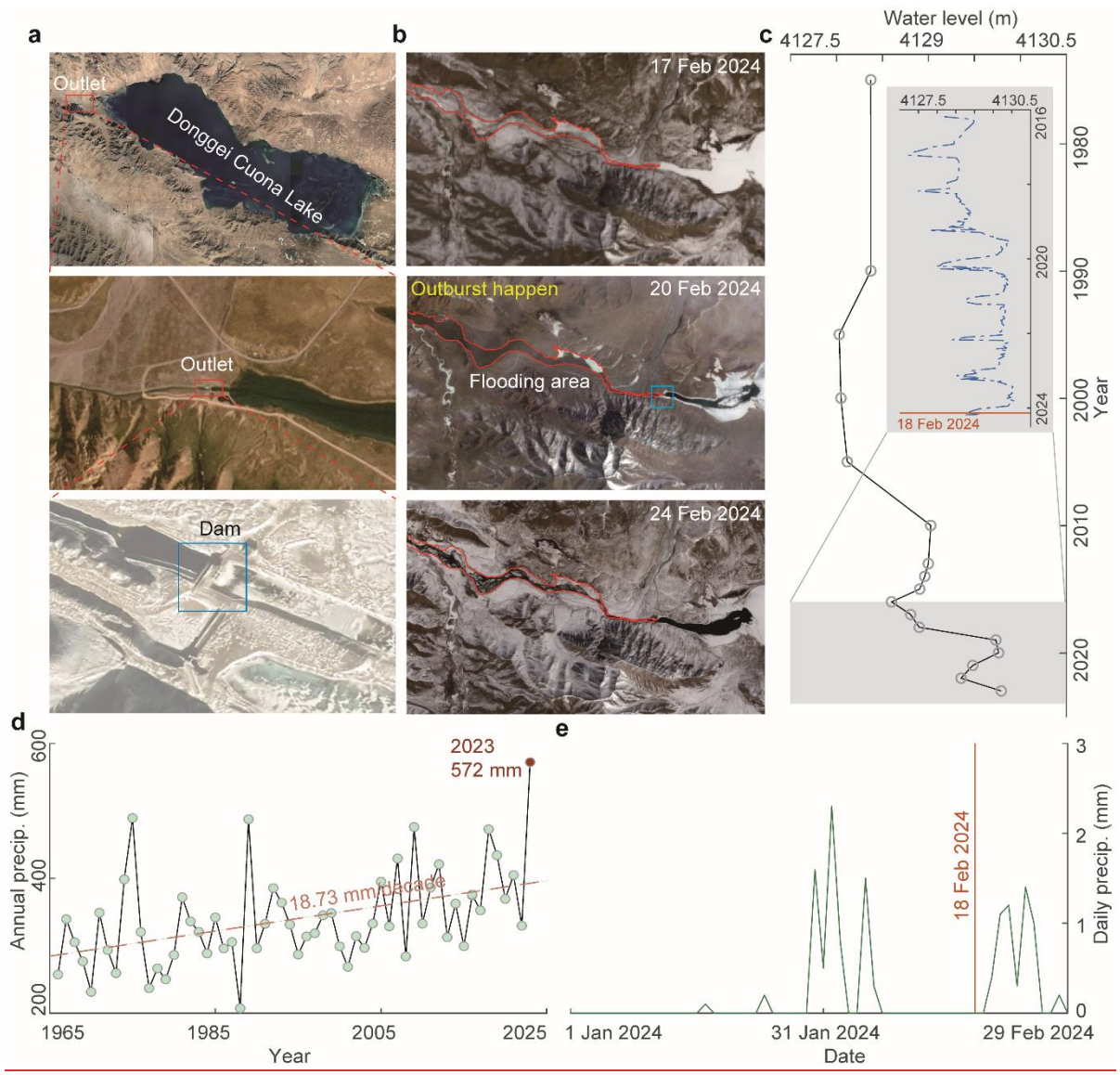
4.2 Consequences of Zonag Lake and Selin Co outburst

Zonag Lake outburst has resulted in a cascade of consequences (Figure 3a). The ongoing expansion of the Yanhu Lake directly threatens the safety of the nearby Qinghai-Tibet Railway and highway (Lu et al., 2021). As a result, an artificial diversion channel was constructed for the Yanhu Lake in 2019 to channel water into the Yangtze Basin. Furthermore, this event accelerated the degradation of the permafrost surrounding the Yanhu Lake (Lu et al., 2020a) and facilitated the formation of new permafrost on the exposed lakebed of Zonag Lake (Zhang et al., 2022). The shrinkage of Zonag Lake directly caused sandstorms, exacerbating desertification (Lu et al., 2020b). Additionally, the connectivity between Zonag Lake and Kusai Lake, along with the erosion of river channels, has hindered the migration and reproduction of the Tibetan antelope (Liu et al., 2016).

The Floodwaters of Selin Co flowed into Bango through the newly formed channel, merging the two basins into one and temporarily changing Selin Co from an endorheic to an exorheic lake (Figure 45). In addition, the Selin Co flood eroded the soil and carried substantial sediment into Bange Co, muddying its waters. Bange Co contains large quantities of high grade LiCl (lithium chloride), well above industry standards, and has significant development potential (Li et al., 2024). However, the continued inflow of Selin Co floodwater had diluted the concentration of LiCl in Bange Co, increasing production costs and reducing economic value. The damaged section of the road is located south of an intersection, disrupting travel on both two roads, and severely impacting the daily lives of residents. Local traffic was restored on 25 October following emergency repairs by government authorities by sealing the breach and building temporary roads.bridges. In addition, water in Selin Co has reachedreached the road on its southeastern side in October 2023 and is threatening to flood it -(Figure 3b).

4.3 Signs and recommendations for recent increasing lake outbursts

On 18 February 2024, the Donggei Cuona Lake in Qinghai Province experienced a burst in the floodgate on the left side of its dam due to its expansion (Figure 1312). Donggei Cuona Lake is an artificially influenced exorheic lake, with a dam constructed at its eastern outlet. It is important to emphasis that this outburst event occurred in winter when the lake surface was fully frozen. The area of Donggei Cuona Lake has increased by 14% from 229 ± 1.40 km^2 in 2000 to 260 ± 3.33 km^2 in 2023, and the water level has risen by 1.75 m, which is mainly attributed to the significant increase in precipitation. The nearest weather station to the Donggei Cuona Lake indicates that precipitation in 2023 reached 572 mm, setting the highest record in the past 60 years, compared to a historical average of 340 mm. This outburst resulted in a significant increase in discharge pressure in the downstream river channels, which had substantial impacts on human living environments, affecting five townships and resulting in the death of approximately 195 livestock. Additionally, about 24.95 km of roads and pastoral paths and some water management facilities were destroyed by flooding, and some pastures were also inundated. Emergency repairs were promptly undertaken, and the damaged gate was sealed on 21 February (Wang, 2024).
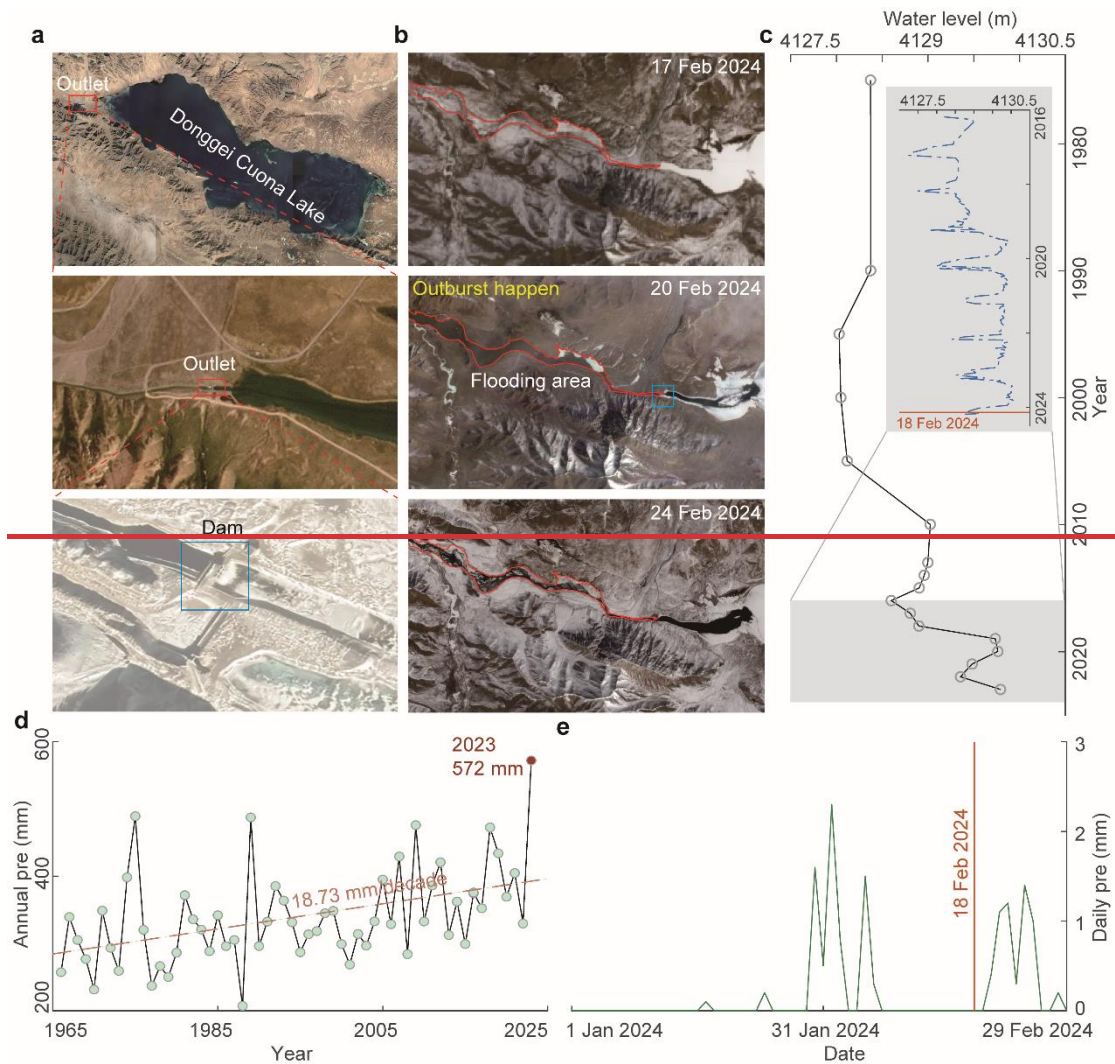
31

a

Outlet

Donggei Cuona Lake

Outlet

Dam

b

17 Feb 2024

Outburst happen   20 Feb 2024

Flooding area

24 Feb 2024

c

Water level (m)

4127.5   4129   4130.5

4127.5   4130.5

1980

1990

2000

2010

2020

Year

18 Feb 2024

2016

2024

d

2023
572 mm

18.73 mm/decade

Annual precip. (mm)

1965   1985   2005   2025

Year

e

18 Feb 2024

1 Jan 2024   31 Jan 2024   29 Feb 2024

Date

Daily precip. (mm)

Figure ~~13~~12. The location, outbrust process, and area change of Donggei Cuona lake. (**a**) The location, outlets, and dams of lakes. (**b**) The outbrust process based on the Landsat imagery on (17 February 2024~~)~~, PlanetScope on (20 February 2024~~)~~ and Sentinel-2 on (24 February 2024~~) imagery~~. (**c**) The change in lake water level from 1975 to 2023. The inset shows the water level change derived from Sentinel-3 data. (**d**) The change of annual precipitation from the Maduo weather station near Donggei Cuona Lake. (**e**) The daily precipitation from 1 January to 29 February 2024.

The outburst of Zonag Lake and Selin Co occurred in September, at the end of the monsoon season, indicating that lakes are at a higher risk of outburst following the expansion of lakes due to continuous rainfall during the monsoon period. In contrast, the outburst of Donggei Cuona Lake in winter exhibited distinct characteristics from the monsoon season. The occurrence of this event while the lake surface remained entirely frozen suggests other factors facilitating the outburst, including vulnerabilities in the dam structure, sustained pressure on the dam due to rising water levels, and groundwater recharge in winter (Lei et al., 2022). The lake outburst outside the monsoon period may yield unexpected impacts on the surrounding environment and infrastructure, necessitating further in-depth research and monitoring to mitigate potential risks.

Lake outburst events on the TP can be divided into two categories based on their driving mechanisms: endorheic lake outbursts and ~~glacial lake outburst floods (~~GLOFs~~)~~. The two documented endorheic lake outburst events in this region, Zonag Lake and Selin Co, both involved lakes expanding due to increased water

input until they overflowed. This overflow led to erosion at the breach site, eventually resulting in full outbursts. For instance, in the Selin Co event, the breach widened from ~ 60 m on 23 September 2024 to ~200 m on 8 October 2024 due to ongoing erosion, which illustrates how overflow can rapidly escalate into a breach. In contrast, GLOFs are typically triggered by external factors such as ice avalanches and, landslides. These events cause rapid destabilization of glacial lakes, leading to sudden, high-discharge floods that peak within hours or cause the end of flood releases. GLOFs tend to be more frequent due to the unstable nature of glacierals and other factors. For example, the Gongbatongsha Co outburst events in 2016 in China demonstrate the devastating potential of these sudden releases (Wang et al., 2024), which are often difficult to predict and have higher peak discharge compared to endorheic lake outbursts.

While both types of events pose significant risks, endorheic lake outbursts are more gradual in nature, driven by the internal dynamics of lake expansion. In contrast, GLOFs are driven by external forces, often resulting in more abrupt and catastrophic flooding. Understanding these differences is critical for risk assessment and management on the TPibetan Plateau, as the two types of lakes require different monitoring and mitigation approaches. For instance, monitoring glacier dynamics and potential ice avalanches is crucial for GLOFs, whereas tracking lake water levels and identifying potential overflow points is key for managing endorheic lake outbursts. In the future, The lakes on the TP are expected to projected to continue to expand in the future (Yang et al., 2018; Liu and Chen, 2022), which will further increase the challenge of lake outburst mitigation. The widespread or synchronous nature of lake expansion on the TP means that there is enormous pressure to mitigate lake outbursts (Zhang et al., 2017b). In the future, lakes on the TP are projected to expand (Yang et al., 2018; Liu and Chen, 2022), which will further increase the challenge of lake outburst mitigation. Therefore, it is necessary to strengthen the risk assessment of existing lakes and develop more effective disaster prevention and mitigation strategies, including improvement of monitoring and early warning systems, the reinforcement of lake embankments, and enhance of the emergency response capacity. At the same time, it is also necessary to conduct in-depth studies on the relationship between lake expansion and outburst events and strengthen prediction studies to better protect the ecological environment and the safety of people's lives and property on the TP and to promote sustainable development.

5 Conclusions

The TP is home to the highest and most numerous groups of high-attitude lakes on Earth, which have experienced significant expansion. From the 1970s to 2023, the number and area of lakes larger than 1 km^2 increased by ~42% and ~29%, respectively. In particular, the number and area of lakes in 2023 have reached new levelshighs for the last 50 years, with 1,537 lakes larger than 1 km^2 and a total area of 51,928±853 km^2, showing an extreme expansion. The continued expansion of the lakes has led to increasing signs of outbursts, from Zonag Lake on 15 September 2011 to Selin Co on 23 21 September 2023 and Donggei Cuona Lake on 18 February 2024.

The Zonag Lake outburst resulted in a significant area reduction of ~45%, while the Yanhu Lake expanded dramatically by ~347% from 2011 to 2023. The Selin Co outburst caused a 2.3 m rise in the water level and an 18% increase in areathe area of downstream Bange Co within 21 23 days, while the water level of Selin Co decreased by only ~0.12 m. Both Zonag Lake and Selin Co are endorheic lakes that expanded to the maximum capacity allowed by their surrounding terrain before the outburst. However, although the area of Zonag Lake is relatively small compared to Selin Co, the steep terrain and large fracture facilitated a rapid average discharge of ~2,1912,238 m³/s, whereas the Selin Co outburst discharged more slowly at ~154170 m³/s due to the flat topography of the fracture. Selin Co caused only a short period of basin reorganization due to human intervention, in contrast to Zonag Lake, which caused a permanent reorganization.

Lake outbursts are mainly due to a long-term increase in precipitation, while an increase in extreme precipitation events also accelerates the early onset of outbursts. The increase in precipitation is mainly attributed to enhanced vertical moisture advection. Thermodynamic effects dominated Zonag Lake, highlighting the important role of climate-induced increases in water content. In contrast, dynamic effects were the primary cause of increased precipitation in the Selin Co basin, indicating the dominance of vertical motions driven by changes in atmospheric circulation. Despite anthropogenic intervention in Donggei Cuona Lake, the rising water level due to increased precipitation also had a significant impact on the breach.

These lake outbursts had a cascade of consequences, such as the destruction of the S208 road by the flooding of Selin Co, the rapid expansion of the tailwater lake, the flooding of inundation of pastures, the death of livestock, the accelerated permafrost degradation, and the reorganization of the drainage system. The recent increase in lake outburst events suggests that lake outbursts on the TP may become more frequent and widespread in the future as lakes continue to expand. Therefore, prediction of future lake changes and potential outbursts is~~are~~ urgently needed.

Author contributions. G. Zhang designed the concept of this study. F. Xu drafted the manuscript. All authors reviewed and edited the final manuscript.

References

Chen, W., Yao, T., Zhang, G., Li, S., and Zheng, G.: Accelerated glacier mass loss in the largest river and lake source regions of the Tibetan Plateau and its links with local water balance over 1976–2017, J Glaciol, 67, 577-591,
715   https://doi.org/10.1017/jog.2021.9, 2021a.

Chen, W., Liu, Y., Zhang, G., Yang, K., Zhou, T., Wang, J., and Shum, C. K.: What Controls Lake Contraction and Then Expansion in Tibetan Plateau's Endorheic Basin Over the Past Half Century?, Geophysical Research Letters, 49, e2022GL101200, https://doi.org/10.1029/2022gl101200, 2022.

Chen, Y., Lu, S., Zhou, J., Baig, M. H. A., Chen, F., Tang, H., Zhang, Y., Yang, X., and Ge, L.: Hydrological ecosystem
720   changes and impacts after the Zonag Lake outburst in Hoh Xil of Tibetan Plateau, Journal of Asian Earth Sciences: X, 6, 100064, https://doi.org/10.1016/j.jaesx.2021.100064, 2021b.

Crétaux, J. F., Abarca-del-Río, R., Bergé-Nguyen, M., Arsen, A., Drolon, V., Clos, G., and Maisongrande, P.: Lake Volume Monitoring from Space, Surveys in Geophysics, 37, 269-305, https://doi.org/10.1007/s10712-016-9362-6, 2016.

Crétaux, J. F., Arsen, A., Calmant, S., Kouraev, A., Vuglinski, V., Bergé-Nguyen, M., Gennero, M. C., Nino, F., Abarca Del
725   Rio, R., Cazenave, A., and Maisongrande, P.: SOLS: A lake database to monitor in the Near Real Time water level and storage variations from remote sensing data, Advances in Space Research, 47, 1497-1507, https://doi.org/10.1016/j.asr.2011.01.004, 2011.

Hersbach, H., Bell, B., Berrisford, P., Hirahara, S., Horányi, A., Muñoz-Sabater, J., Nicolas, J., Peubey, C., Radu, R., Schepers, D., Simmons, A., Soci, C., Abdalla, S., Abellan, X., Balsamo, G., Bechtold, P., Biavati, G., Bidlot, J., Bonavita,
730   M., De Chiara, G., Dahlgren, P., Dee, D., Diamantakis, M., Dragani, R., Flemming, J., Forbes, R., Fuentes, M., Geer, A., Haimberger, L., Healy, S., Hogan, R. J., Hólm, E., Janisková, M., Keeley, S., Laloyaux, P., Lopez, P., Lupu, C., Radnoti, G., de Rosnay, P., Rozum, I., Vamborg, F., Villaume, S., and Thépaut, J. N.: The ERA5 global reanalysis, Quarterly Journal of the Royal Meteorological Society, 146, 1999-2049, https://doi.org/10.1002/qj.3803, 2020.

Lei, Y., Yang, K., Wang, B., Sheng, Y., Bird, B. W., Zhang, G., and Tian, L.: Response of inland lake dynamics over the
735   Tibetan Plateau to climate change, Climatic Change, 125, 281-290, https://doi.org/10.1007/s10584-014-1175-3, 2014.

Lei, Y., Yang, K., Immerzeel, W. W., Song, P., Bird, B. W., He, J., Zhao, H., and Li, Z.: Critical role of groundwater inflow in sustaining lake water balance on the western Tibetan Plateau, Geophys Res Lett, 49, e2022GL099268, https://doi.org/10.1029/2022GL099268, 2022.

740 Lei, Y., Zhu, Y., Wang, B., Yao, T., Yang, K., Zhang, X., Zhai, J., and Ma, N.: Extreme lake level changes on the Tibetan Plateau associated with the 2015/2016 El Niño, Geophys Res Lett, 46, 5889-5898, https://doi.org/10.1029/2019gl081946, 2019.

Lei, Y., Yao, T., Sheng, Y., Yang, K., Yang, W., Li, S., Zhou, J., Jiang, Y., and Yu, Y.: Unprecedented lake expansion in 2017–2018 on the Tibetan Plateau: Processes and environmental impacts, Journal of Hydrology, 619, 129333,
745   https://doi.org/10.1016/j.jhydrol.2023.129333, 2023.

Lei, Y., Zhou, J., Yao, T., Bird, B. W., Yu, Y., Wang, S., Yang, K., Zhang, Y., Zhai, J., and Dai, Y.: Overflow of Siling Co on the central Tibetan Plateau and its environmental impacts, Sci Bull, https://doi.org/10.1016/j.scib.2024.07.035, 2024.

Li, S., Ye, C., and Zhao, Y.: Prediction about water level variations of lithium-rich salt lake in Bankog Co，Xizang,
750   Journal of Salt Lake Research, 32, 39-47, https://doi.org/10.12119/j.yhyj.202401005, 2024.

Li, X., Long, D., Scanlon, B. R., Mann, M. E., Li, X., Tian, F., Sun, Z., and Wang, G.: Climate change threatens terrestrial water storage over the Tibetan Plateau, Nature Climate Change, 12, 801-807, https://doi.org/10.1038/s41558-022-01443-0, 2022.

Liu, B., Du, Y. e., Li, L., Feng, Q., Xie, H., Liang, T., Hou, F., and Ren, J.: Outburst Flooding of the Moraine-Dammed Zhuonai Lake on Tibetan Plateau: Causes and Impacts, IEEE Geoscience and Remote Sensing Letters, 13, 570-574, https://doi.org/10.1109/lgrs.2016.2525778, 2016.

Liu, W., Xie, C., Zhao, L., Wu, T., Wang, W., Zhang, Y., Yang, G., Zhu, X., and Yue, G.: Dynamic changes in lakes in the Hoh Xil region before and after the 2011 outburst of Zonag Lake, Journal of Mountain Science, 16, 1098-1110, https://doi.org/10.1007/s11629-018-5085-0, 2019.

Liu, Y. and Chen, H.: Future warming accelerates lake variations in the Tibetan Plateau, Int J Climatol, 42, 8687-8700, https://doi.org/10.1002/joc.7760, 2022.

Liu, Y., Chen, H., Li, H., Zhang, G., and Wang, H.: What induces the interdecadal shift of the dipole patterns of summer precipitation trends over the Tibetan Plateau?, International Journal of Climatology, 41, 5159–5177, https://doi.org/10.1002/joc.7122, 2021.

Liu, Y., Wang, H., Chen, H., Zhang, Z., Li, H., and Liu, B.: Anthropogenic forcing and Pacific internal variability-determined decadal increase in summer precipitation over the Asian water tower, npj Climate and Atmospheric Science, 6, 38, https://doi.org/10.1038/s41612-023-00369-4, 2023.

Loewen, C. J. G.: Lakes as model systems for understanding global change, Nature Climate Change, 13, 304-306, https://doi.org/10.1038/s41558-023-01624-5, 2023.

Lu, P., Han, J., Li, Z., Xu, R., Li, R., Hao, T., and Qiao, G.: Lake outburst accelerated permafrost degradation on Qinghai-Tibet Plateau, Remote Sensing of Environment, 249, 112011, https://doi.org/10.1016/j.rse.2020.112011, 2020a.

Lu, S., Chen, F., Zhou, J., Hughes, A. C., Ma, X., and Gao, W.: Cascading implications of a single climate change event for fragile ecosystems on the Qinghai-Tibetan Plateau, Ecosphere, 11, e03243, https://doi.org/10.1002/ecs2.3243, 2020b.

Lu, S., Jin, J., Zhou, J., Li, X., Ju, J., Li, M., Chen, F., Zhu, L., Zhao, H., Yan, Q., Xie, C., Yao, X., and Fagherazzi, S.: Drainage basin reorganization and endorheic-exorheic transition triggered by climate change and human intervention, Global Planet Change, 201, 103494, https://doi.org/10.1016/j.gloplacha.2021.103494, 2021.

Ma, R., Duan, H., Hu, C., Feng, X., Li, A., Ju, W., Jiang, J., and Yang, G.: A half-century of changes in China's lakes: Global warming or human influence?, Geophysical Research Letters, 37, L24106, https://doi.org/10.1029/2010gl045514, 2010.

McFeeters, S. K.: The use of the Normalized Difference Water Index (NDWI) in the delineation of open water features, International Journal of Remote Sensing, 17, 1425-1432, https://doi.org/10.1080/01431169608948714, 1996.

Mullen, A. L., Watts, J. D., Rogers, B. M., Carroll, M. L., Elder, C. D., Noomah, J., Williams, Z., Caraballo-Vega, J. A., Bredder, A., Rickenbaugh, E., Levenson, E., Cooley, S. W., Hung, J. K. Y., Fiske, G., Potter, S., Yang, Y., Miller, C. E., Natali, S. M., Douglas, T. A., and Kyzivat, E. D.: Using High-Resolution Satellite Imagery and Deep Learning to Track Dynamic Seasonality in Small Water Bodies, Geophysical Research Letters, 50, https://doi.org/10.1029/2022gl102327, 2023.

Otsu, N.: A Threshold Selection Method from Gray-Level Histograms, IEEE Transactions on Systems, Man, and Cybernetics, 9, 62-66, https://doi.org/10.1109/TSMC.1979.4310076, 1979.

Pokhrel, Y., Felfelani, F., Satoh, Y., Boulange, J., Burek, P., Gädeke, A., Gerten, D., Gosling, S. N., Grillakis, M., Gudmundsson, L., Hanasaki, N., Kim, H., Koutroulis, A., Liu, J., Papadimitriou, L., Schewe, J., Müller Schmied, H., Stacke, T., Telteu, C.-E., Thiery, W., Veldkamp, T., Zhao, F., and Wada, Y.: Global terrestrial water storage and drought severity under climate change, Nature Climate Change, 11, 226-233, https://doi.org/10.1038/s41558-020-00972-w, 2021.

Song, C., Huang, B., and Ke, L.: Modeling and analysis of lake water storage changes on the Tibetan Plateau using multi-mission satellite data, Remote Sensing of Environment, 135, 25-35, https://doi.org/10.1016/j.rse.2013.03.013, 2013.

Sun, J., Yang, K., Guo, W., Wang, Y., He, J., and Lu, H.: Why Has the Inner Tibetan Plateau Become Wetter since the Mid-1990s?, Journal of Climate, 33, 8507-8522, https://doi.org/10.1175/jcli-d-19-0471.1, 2020.

Takaya, K. and Nakamura, H.: A Formulation of a Phase-Independent Wave-Activity Flux for Stationary and Migratory Quasigeostrophic Eddies on a Zonally Varying Basic Flow, J Atmos Sci, 58, 608-627, https://doi.org/10.1175/1520-0469(2001)058<0608:Afoapi>2.0.Co;2, 2001.

Tong, K., Su, F., and Xu, B.: Quantifying the contribution of glacier meltwater in the expansion of the largest lake in Tibet, Journal of Geophysical Research: Atmospheres, 121, https://doi.org/10.1002/2016jd025424, 2016.

Veh, G., Korup, O., and Walz, A.: Hazard from Himalayan glacier lake outburst floods, Proc Natl Acad Sci U S A, 117, 907-912, https://doi.org/10.1073/pnas.1914898117, 2020.

Flooding in Qinghai Province? Official response: not consistent with the facts did not cause casualties https://news.cctv.com/2024/03/02/ARTIwBthTZFUklWgPzCIQmOu240302.shtml, last access: 15 October 2024~~-10-15~~.

Wang, L., Liu, H., Zhong, X., Zhou, J., Zhu, L., Yao, T., Xie, C., Ju, J., Chen, D., and Yang, K.: Domino effect of a natural cascade alpine lake system on the Third Pole, PNAS nexus, 1, pgac053, https://doi.org/10.1093/pnasnexus/pgac053, 2022a.

Wang, L., Zhao, L., Zhou, H., Liu, S., Du, E., Zou, D., Liu, G., Xiao, Y., Hu, G., Wang, C., Sun, Z., Li, Z., Qiao, Y., Wu, T., Li, C., and Li, X.: Contribution of ground ice melting to the expansion of Selin Co (lake) on the Tibetan Plateau, The Cryosphere, 16, 2745-2767, https://doi.org/10.5194/tc-16-2745-2022, 2022b.

Wang, X., Zhang, G., Veh, G., Sattar, A., Wang, W., Allen, S. K., Bolch, T., Peng, M., and Xu, F.: Reconstructing glacial lake outburst floods in the Poiqu River basin, central Himalaya, Geomorphology, 449, https://doi.org/10.1016/j.geomorph.2024.109063, 2024.

Xu, F., Zhang, G., Yi, S., and Chen, W.: Seasonal trends and cycles of lake-level variations over the Tibetan Plateau using multi-sensor altimetry data, Journal of Hydrology, 604, 127251, https://doi.org/10.1016/j.jhydrol.2021.127251, 2021.

Xu, F., Zhang, G., Woolway, R. I., Yang, K., Wada, Y., Wang, J., and Crétaux, J.-F.: Widespread societal and ecological impacts from projected Tibetan Plateau lake expansion, Nature Geoscience, 17, 516–523, https://doi.org/10.1038/s41561-024-01446-w, 2024.

Yang, K., Lu, H., Yue, S., Zhang, G., Lei, Y., La, Z., and Wang, W. J. C. C.: Quantifying recent precipitation change and predicting lake expansion in the Inner Tibetan Plateau, Climatic Change 147, 149-163, https://doi.org/10.1007/s10584-017-2127-5, 2018.

Yang, X., Qin, Q., Yésou, H., Ledauphin, T., Koehl, M., Grussenmeyer, P., and Zhu, Z.: Monthly estimation of the surface water extent in France at a 10-m resolution using Sentinel-2 data, Remote Sens Environ, 244, https://doi.org/10.1016/j.rse.2020.111803, 2020.

Yi, S., Wang, Q., and Sun, W.: Basin mass dynamic changes in China from GRACE based on a multibasin inversion method, Journal of Geophysical Research: Solid Earth, 121, 3782-3803, https://doi.org/10.1002/2015jb012608, 2016.

Zhang, G., Bolch, T., Chen, W., and Cretaux, J. F.: Comprehensive estimation of lake volume changes on the Tibetan Plateau during 1976-2019 and basin-wide glacier contribution, Sci. Total Environ., 772, 145463, https://doi.org/10.1016/j.scitotenv.2021.145463, 2021.

Zhang, G., Luo, W., Chen, W., and Zheng, G.: A robust but variable lake expansion on the Tibetan Plateau, Science Bulletin, 64, 1306-1309, https://doi.org/10.1016/j.scib.2019.07.018, 2019a.

Zhang, G., Yao, T., Chen, W., Zheng, G., Shum, C. K., Yang, K., Piao, S., Sheng, Y., Yi, S., Li, J., O'Reilly, C. M., Qi, S., Shen,
840   S. S. P., Zhang, H., and Jia, Y.: Regional differences of lake evolution across China during 1960s–2015 and its
       natural   and   anthropogenic   causes,   Remote   Sens   Environ,   221,   386-404,
       https://doi.org/10.1016/j.rse.2018.11.038, 2019b.

Zhang, G. Q., Li, J. L., and Zheng, G. X.: Lake-area mapping in the Tibetan Plateau: an evaluation of data and methods,
       International Journal of Remote Sensing, 38, 742-772, https://doi.org/10.1080/01431161.2016.1271478, 2017a.

845 Zhang, G. Q., Yao, T. D., Shum, C. K., Yi, S., Yang, K., Xie, H. J., Feng, W., Bolch, T., Wang, L., Behrangi, A., Zhang, H. B.,
       Wang, W. C., Xiang, Y., and Yu, J. Y.: Lake volume and groundwater storage variations in Tibetan Plateau's
       endorheic basin, Geophysical Research Letters, 44, 5550-5560, https://doi.org/10.1002/2017gl073773, 2017b.

Zhang, Y., Xie, C., Wu, T., Zhao, L., Wu, J., Wu, X., Li, R., Hu, G., Liu, G., Wang, W., and Yang, G.: New permafrost is
       forming on the exposed bottom of Zonag Lake on the Qinghai-Tibet Plateau, The Science of the total
850   environment, 815, 152879, https://doi.org/10.1016/j.scitotenv.2021.152879, 2022.

Zheng, G., Allen, S. K., Bao, A., Ballesteros-Cánovas, J. A., Huss, M., Zhang, G., Li, J., Yuan, Y., Jiang, L., Yu, T., Chen, W.,
       and Stoffel, M.: Increasing risk of glacial lake outburst floods from future Third Pole deglaciation, Nature Climate
       Change, 11, 411-417, https://doi.org/10.1038/s41558-021-01028-3, 2021.

Zhou, J., Wang, L., Zhong, X., Yao, T., Qi, J., Wang, Y., and Xue, Y.: Quantifying the major drivers for the expanding
855   lakes in the interior Tibetan Plateau, Science Bulletin, 67, 474-478, https://doi.org/10.1016/j.scib.2021.11.010,
       2021.